Inorganic Chemistry

ARTICLE

pubs.acs.org/IC

o-Iminobenzosemiquinonate and *o*-Imino-*p*-methylbenzosemiquinonate Anion Radicals Coupled VO^{2+} Stabilization

Amit Saha Roy,[†] Pinaki Saha,[†] Nirmal Das Adhikary,[‡] and Prasanta Ghosh*[,†]

[†]Department of Chemistry, R. K. Mission Residential College, Narendrapur, Kolkata-103, India

[‡]Indian Institute of Chemical Biology, Jadavpur, Kolkata-32, India

Supporting Information

ABSTRACT:

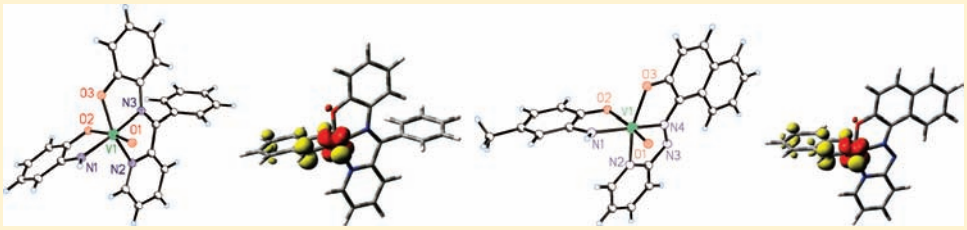

The diamagnetic VO^{2+}-iminobenzosemiquinonate anion radical ($L^{R}_{IS}{}^{\bullet-}$, R = H, Me) complexes, $(L^{-})(VO^{2+})(L^{R}_{IS}{}^{\bullet-})$: $(L_1{}^{-})(VO^{2+})(L^{H}_{IS}{}^{\bullet-})\bullet 3/2MeOH$ (**1**•3/2MeOH), $(L_2{}^{-})(VO^{2+})(L^{H}_{IS}{}^{\bullet-})$ (**2**), and $(L_2{}^{-})(VO^{2+})(L^{Me}_{IS}{}^{\bullet-})\bullet 1/2\ L^{Me}_{AP}$ (**3**•1/2 L^{Me}_{AP}), incorporating tridentate monoanionic NNO-donor ligands {L = $L_1{}^{-}$ or $L_2{}^{-}$, L_1H = (2-[(phenylpyridin-2-yl-methylene)amino]phenol; L_2H = 1-(2-pyridylazo)-2-naphthol; $L^{H}_{IS}{}^{\bullet-}$ = *o*-iminobenzosemiquinonate anion radical; $L^{Me}_{IS}{}^{\bullet-}$ = *o*-imino-*p*-methylbenzosemiquinonate anion radical; and L^{Me}_{AP} = *o*-amino-*p*-methylphenol} have been isolated and characterized by elemental analyses, IR, mass, NMR, and UV−vis spectra, including the single-crystal X-ray structure determinations of **1**•3/2MeOH and **3**•1/2 L^{Me}_{AP}. Complexes **1**•3/2MeOH, **2**, and **3**•1/2 L^{Me}_{AP} absorb strongly in the visible region because of intraligand (IL) and ligand-to-metal charge transfers (LMCT). **1**•3/2MeOH is luminescent (λ_{ext}, 333 nm; λ_{em}, 522, 553 nm) in frozen dichloromethane−toluene glass at 77 K due to $\pi_{diimine} \rightarrow \pi_{diimine}{}^{*}$ transition. The $V-O_{phenolato}$ (*cis* to the V═O) lengths, 1.940(2) and 1.984(2) Å, respectively, in **1**•3/2MeOH and **3**•1/2 L^{Me}_{AP} are consistent with the VO^{2+} description. The $V-O_{iminosemiquinonate}$ (*trans* to the V═O) lengths, 2.1324(19) in **1**•3/2MeOH and 2.083(2) Å in **3**•1/2 L^{Me}_{AP}, are expectedly ∼0.20 Å longer due to the *trans* influence of the V═O bond. Because of the stronger affinity of the paramagnetic VO^{2+} ion to the $L^{H}_{IS}{}^{\bullet-}$ or $L^{Me}_{IS}{}^{\bullet-}$, the $V-N_{iminosemiquinonate}$ lengths, 1.908(2) and 1.921(2) Å, respectively, in **1**•3/2MeOH and **3**•1/2 L^{Me}_{AP}, are unexpectedly shorter. Density functional theory (DFT) calculations using B3LYP, B3PW91, and PBE1PBE functionals on **1** and **2** have established that *the closed shell singlet (CSS) solutions (VO^{3+}-amidophenolato ($L^{R}_{AP}{}^{2-}$) coordination) of these complexes are unstable with respect to triplet perturbations*. But BS (1,1) $M_s = 0$ (VO^{2+}-iminobenzosemiquinonate anion radical ($L^{R}_{IS}{}^{\bullet-}$) coordination) solutions of these species are stable and reproduce the experimental bond parameters well. Spin density distributions of one electron oxidized cations are consistent with the $[(L^{-})(VO^{2+})(L^{R}_{IQ})]^{+}$ descriptions [VO^{2+}-*o*-iminobenzoquinone (L^{R}_{IQ}) coordination], and one electron reduced anions are consistent with the $[(L^{\bullet 2-})(VO^{3+})(L^{R}_{AP}{}^{2-})]^{-}$ descriptions [VO^{3+}-amidophenolato ($L^{R}_{AP}{}^{2-}$) coordination], incorporating the diimine anion radical ($L_1{}^{\bullet 2-}$) or azo anion radical ($L_2{}^{3-}$). Although, cations and anions are not isolable, but electro-and spectro-electrochemical experiments have shown that $\mathbf{3}^{+}$ and $\mathbf{3}^{-}$ ions are more stable than $\mathbf{1}^{+}$, $\mathbf{2}^{+}$ and $\mathbf{1}^{-}$, $\mathbf{2}^{-}$ ions. In all cases, the reductions occur with simultaneous two electron transfer, may be due to formation of coupled diimine/azo anion radical-VO^{2+} species as in $[(L^{\bullet 2-})(VO^{2+})(L^{R}_{AP}{}^{2-})]^{2-}$.

1. INTRODUCTION

Chemical researchers have been intrigued by the biological role of vanadium compounds.[1] The existence of vanadate-dependent haloperoxidases,[2] vanadium−nitrogenase[3] that catalyze multi-electron transfer reactions, vanabins[4] and vanadates that alleviate diabetes mellitus symptoms[5] and are used potent inhibitors of several phosphate-metabolizing enzymes,[6] like ribonucleases, mutases, and phosphatases, have inspired scientists to mimic the same enzymatic and medicinal activities with model coordination compounds of vanadium synthesized in the laboratory.[7] The investigations have revealed that the bioactivity of vanadium depends on its oxidation state,[1,7] and in this context, we have been persuaded to study the electron transfer series of oxidovanadium complexes with redox non-innocent *o*-aminophenolato ligands. Oxidovanadium complexes with redox active

Received: November 17, 2010
Published: February 24, 2011

Chart 1

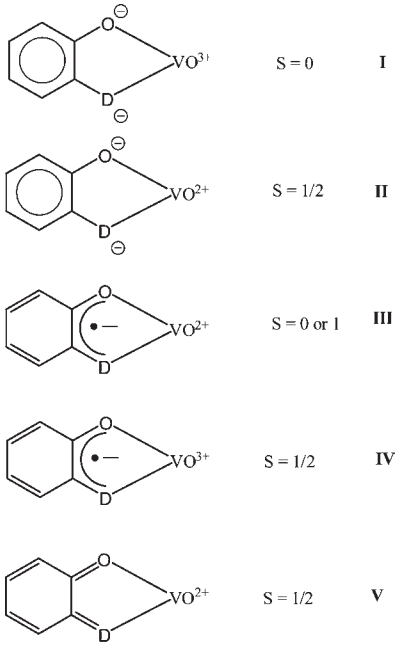

organic ligands, particularly catecholate,[8] *p*-hydroquinone,[9] 2-anilino-4,6-di-*tert*-butylphenol, and its derivative[10] that undergo multi-electron transfer, have been investigated in many aspects. The impact of VO^{2+} and VO^{3+}, two active oxidovanadium cores, the former being one electron paramagnetic, with a paramagnetic benzosemiquinonate or iminobenzosemiquinonate anion radical, has been worth analyzing. Two $VO^{2+/3+}$ cores potentially can afford four types of binding with dianionic catecholato types and monoanionic *o*-benzosemiquinonate or *o*-iminobenzosemiquinonate radicals as in Chart 1. In the literature, only the species of type I with D = O, i.e., catecholate species of VO^{3+}, have been reported,[8] and surprisingly, not a single species incorporating II, III, IV, or V chelate has been authenticated so far. In most cases, *o*-aminophenolates produce nonoxido vanadium species except one with a modified penta-dentate aminophenol ligand.[10a]

Recently, Keramidas et al. found a stronger affinity of the *p*-benzosemiquinonate anion radical toward the paramagnetic $V^{IV}O$ ion in a series of binuclear and tetranuclear OV^{V} and OV^{IV} skeletons incorporating redox non-innocent 2,5-bis[N,N-bis-(carboxymethyl)aminomethyl]hydroquinone, a dinucleating ligand.[9] The work disclosed that the $V^{IV}-O_{semiquinonate}$ bond is stronger than the $V^{IV}-O_{catecholato}$ bond. In this work, we have successfully augmented this novel chemistry with *o*-aminophenol (D = NH) ligands by reporting coordination type III, i.e., an *o*-imino-*p*-R-benzosemiquinonate anion radical ($L^{R}_{IS}{}^{\bullet-}$, R = H, Me) coordinated to a VO^{2+} core as in $(L^{-})(VO^{2+})(L^{R}_{IS}{}^{\bullet-})$: $(L_1{}^{-})(VO^{2+})(L^{H}_{IS}{}^{\bullet-})\bullet 3/2MeOH$ (**1**•3/2MeOH), $(L_2-)(VO^{2+})(L^{H}_{IS}{}^{\bullet-})$ (**2**), and $(L_2-)(VO^{2+})(L^{Me}_{IS}{}^{\bullet-})\bullet 1/2\ L^{Me}_{AP}$ (**3**•1/2 L^{Me}_{AP}) {L_1H = (2-[(phenylpyridin-2-yl-methylene)-amino]phenol; L_2H = 1-(2-pyridylazo)-2-naphthol; $L^{H}_{IS}{}^{\bullet-}$ = *o*-iminobenzosemiquinonate anion radical; $L^{Me}_{IS}{}^{\bullet-}$ = *o*-imino-*p*-methylbenzosemiquinonate anion radical; and L^{Me}_{AP} = *o*-amino-*p*-methylphenol}. Both L_1H and L_2H are monodeprotonable

Scheme 1

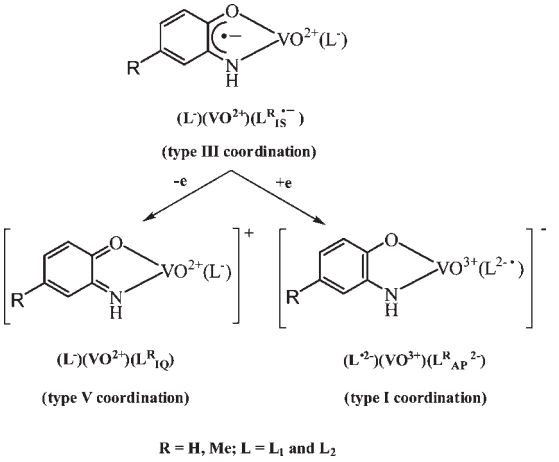

tridentate NNO-donor ligands as shown in Figures 2 and 4. Experimental data and broken symmetry density functional theory (BS DFT) calculations have predicted three types of electron transfer series of these species as shown in Scheme 1.

The investigation has inferred that closed shell singlet (CSS) solutions of these complexes are unstable, and the *o*-imino-*p*-R-benzosemiquinonate anion radical ($L^{R}_{IS}{}^{\bullet-}$)-$V^{IV}O$ spin-coupled ground state (S = 0) stabilizes **1**•3/2MeOH, **2**, and **3**•**1**/2 L^{Me}_{AP} complexes.

2. EXPERIMENTAL SECTION

2.1. Materials and Physical Measurements. Reagents or analytical grade materials were obtained from commercial suppliers and used without further purification. Spectroscopic grade solvents were used for spectroscopic and electrochemical measurements. The synthetic precursor, $VO(acac)_2$, was prepared by the reported procedure.[11] After evaporating MeOH solvents of the sample under high vacuum, elemental analyses and spectral measurements have been performed. The C, H, and N content of the compounds were obtained from a Perkin-Elmer 2400 series II elemental analyzer. Infrared spectra of the samples were measured from 4000 to 400 cm^{-1} with the KBr pellet at room temperature on a Perkin-Elmer Spectrum RX 1, FT-IR spectrophotometer. ^1H NMR spectrum in $CDCl_3$ and DMSO-d solvents were carried out on a Bruker DPX-300 MHz spectrometer with tetramethylsilane (TMS) as an internal reference. ESI mass spectrum was recorded on a micro-mass Q-TOF mass spectrometer. Electronic absorption spectrum in solution at 298 K was carried out on a Perkin-Elmer Lambda 25 spectrophotometer in the range of 1100−200 nm. Magnetic susceptibility at 298 K has been measured on Sherwood magnetic susceptibility balance. Emission spectra at 77 K were recorded in CH_2Cl_2−toluene glass using a quartz sample tube on a Perkin-Elmer LS 55 fluorescence spectrophotometer equipped with a Perkin-Elmer low-temperature luminescence accessory. The electro analytical instrument, BASi Epsilon-EC, has been used for cyclic voltammetric and spectro-electrochemistry experiments.

2.2. Syntheses. *$(L_1{}^{-})(VO^{2+})(L^{H}_{IS}{}^{\bullet-})$•3/2MeOH (1•3/2MeOH).* To a MeOH solution (25 mL) of 2-benzoyl pyridine (366 mg, 2.0 mmol), o-aminophenol (436 mg, 4.0 mmol) was added, and the resulting solution was heated to reflux for 90 min. The reaction mixture was cooled at 40 °C. To this solution $VO(acac)_2$ (534 mg, 2.0 mmol), CH_2Cl_2 (5 mL), and methanol (25 mL) were added successively and allowed to evaporate slowly in air. After 2−3 days, dark brown crystals

dx.doi.org/10.1021/ic102296p |*Inorg. Chem.* 2011, 50, 2488–2500

of **1**•3/2MeOH separated out, which were filtered and dried in air. Yield: 537 mg (60% with respect to vanadium). ESI (positive ion)- MS in CH_3OH; m/z: 448.01($\mathbf{1}^+$). ^1H NMR ($CDCl_3$, 300 MHz, 300 K): δ (ppm) = 14.11(b, N−H), 8.31 (b, 1H), 7.79 (t, 1H), 7.68 (m, 3H), 7.50 (b, 1H), 7.39 (b, 1H), 7.18 (d, 1H), 7.09 (t, 1H), 6.85 (d, 1H), 6.74 (b, 1H), 6.48 (m, 4H), 6.25 (t, 1H), 6.16(d, 1H). Anal. Calcd for $C_{24}H_{18}N_3O_3V$ (**1**): C, 64.43; H, 4.05; N, 9.39. Found: C, 64.32; H, 4.01; N, 9.35. IR (KBr, ν_{max}/cm^{-1}): 3441(m, MeOH), 3210(s, N−H), 1576(vs, CPh=N−), 1548(s), 1475(vs), 1458(vs), 1443(s), 1313(vs), 1269(vs), 1144(vs), 1028(s), 947(vs, V═O), 758(s), 739(s), 706(s), 576(s), 503(m).

*(L_2^-)(VO^{2+})($L^H_{IS}{}^{\bullet-}$) (**2**).* To a MeOH (30 mL) solution of 1-(2-pyridylazo)-2-naphthol (L_2H, 50 mg, 0.2 mmol), 2-aminophenol (22 mg, 0.2 mmol) was added, and the resulting solution was heated at 60 °C for 10−15 min. The solution was cooled to room temperature and filtered. To this filtrated $VO(acac)_2$ (52 mg, 0.2 mmol), CH_2Cl_2 (5 mL) and MeOH (15 mL) were added successively, and the resulting solution was allowed to evaporate slowly in air. After 2−3 days, a dark brown crystalline compound of **2** separated out, which was filtered and dried in air. Yield: 43 mg (51% with respect to vanadium). Mass spectrum (ESI, positive ion, CH_3CN): m/z 423{**2**}$^+$. ^1H NMR (DMSO-d_6, 300 MHz, 300 K): δ (ppm) = 16.19 (s, N−H), 9.31 (d, 1H), 8.23−8.09(m, 3H) 7.92 (t, 2H), 7.75(t, 1H), 7.53(t, 1H), 7.45(t, 1H), 6.97(d, 1H), 6.67 (t, 1H), 6.45(d, 1H), 6.35(t, 1H), 6.22(d, 1H). Anal. Calcd for $C_{21}H_{15}N_4O_3V$: C 59.58, H 3.57, N 13.23. Found: C 59.48, H 3.45, N 13•10. IR (KBr, ν_{max}/cm^{-1}): = 3206(s, N−H), 1588(s, −N═N−), 1507(m), 1473(s), 1355(vs), 1247(vs), 1147(s), 952(vs, V═O), 833(m), 760(m), 557(w), 505(w).

(L_2^-)(VO^{2+})($L^{Me}_{IS}{}^{\bullet-}$).1/2L^{Me}_{AP} (3•1/2L^{Me}_{AP}). This was prepared by the same procedure as **2**, using 1-(2-pyridylazo)-2-naphthol (L_2H, 50 mg, 0.2 mmol), *o*-amino-*p*-methylphenol (L^{Me}_{AP}), 25 mg, 0.2 mmol), and $VO(acac)_2$ (52 mg, 0.2 mmol). Dark brown crystals of **3•1**/2 L^{Me}_{AP} separated out within 2−3 days, incorporating half of a molecule of *o*-amino-*p*-methylphenol (1/2 L^{Me}_{AP}). Single crystals for X-ray structure determinations have been collected from this product. Yield: 55 mg (56% with respect to vanadium). Mass spectrum (ESI, positive ion, CH_3CN): m/z 437{**3**}$^+$. ^1H NMR ($CDCl_3$, 300 MHz, 300 K): δ (ppm) = 15.76 (s, N−H), 13.78 (s, NH_2), 9.35 (d, 1H), 8.41 (d, 1H), 7.91−7.27 (m, 6H), 7.62 (b, 3H), 7.50 (d, 2H), 7.40 (d, 3H), 7.13 (b, 2H), 6.95 (d, 2H), 6.68 (d, 1H), 6.58 (d, 2H), 6.40 (d, 1H), 6.30(s, 1H). Anal. Calcd for $C_{22}H_{17}N_4O_3V.1/2(C_7H_9ON)$: C 61.39, H 4.34, N 12.63. Found: C 61.22, H 4.12, N 12.49. IR (KBr,ν_{max}/cm^{-1}) = 3198(s, N−H), 1605(s), 1587(vs, −N═N−), 1473(vs), 1356(vs), 1327(vs), 1251(vs), 1149v(s), 1018 (s), 937 (vs, V═O), 828(s), 759(m), 553(m), 507(s).

2.3. X-ray Crystallographic Data Collection and Refinement of the Structures. Dark brown single crystals of **1**•3/2MeOH and **3**•1/2 L^{Me}_{AP} were picked up with nylon loops and were mounted on a Bruker Kappa-CCD diffractometer equipped with a Mo target rotating anode X-ray source and a graphite monochromator (Mo Kα, λ = 0.71073 Å). Final cell constants were obtained from least-squares fits of all measured reflections. The structures were readily solved by direct method and subsequent difference Fourier techniques. The crystallographic data of **1**•3/2MeOH and **3**•1/2 L^{Me}_{AP} are listed in Table 1. ShelX97[12] was used for the structure solution and refinement. All non-hydrogen atoms were refined anisotropically, except the L^{Me}_{AP} molecule of **3**•1/2 L^{Me}_{AP}. All the hydrogen atoms were located by a difference Fourier map and refined isotropically. The oxygen atom of one of the MeOH is disordered and has been refined with 50% occupancy. The L^{Me}_{AP} molecule of **3**•1/2 L^{Me}_{AP} is severely disordered with respect to the center of inversion.

2.4. Density Functional Theory (DFT) Calculations. All calculations reported in this article were done with the Gaussian 03W[13] program package supported by GaussView 4.1. The DFT[14] calculations have been performed at the level of Becke three parameter hybrid functional with the nonlocal correlation functional of Lee−Yang−Parr (B3LYP),[15a−c] with the nonlocal correlation provided by Perdew/Wang 91 (B3PW91)[15d−h] and with a hybrid exchange-correlation functional, PBE1PBE.[15i−l] Gas-phase geometries of the hard complexes, **1** and **2**, and a model soft complex, (L_1^-)(VO^{3+})(gly^{2-}) (**4**), have been optimized with Pualy's Direct Inversion[16] in the Iterative Subspace (DIIS), "tight" convergent SCF procedure[17] ignoring symmetry, with singlet and triplet spin states. The geometry of **1** has been optimized with all three functionals for comparison. Stabilities of all the singlet solutions have been checked, and the unstable solutions have been reoptimized. Singlet solutions of all these species are unstable, but the broken symmetry (BS) (1,1) solutions, converging to M_s = 0 solutions, are stable indicating that the open shell electronic structure correlating bond parameters well. Geometries of the cations ($\mathbf{1}^+$, $\mathbf{2}^+$) and anions ($\mathbf{1}^-$, $\mathbf{2}^-$) have been optimized using only a hybrid functional (B3LYP). All the calculations have been performed with a LANL2DZ basis set,[18] along with the corresponding effective core potential (ECP) for vanadium, 6-31G(d,p)[19] basis set for C, O, N atoms, and 6-31G[20] for H atoms. BS DFT calculations have been performed using quadratic SCF convergent. The 60 lowest singlet excitation energies on the optimized geometry of **1** with singlet spin state have been calculated by the TD DFT method.[21] The nature of transitions has been calculated by adding the probability of the same type among the molecular orbitals. Origins and excitation energies of these transitions with oscillator strength greater than 0.04 at 400−600 nm have been analyzed. Analyses have established mainly two types of transitions, intra-L_2^- to L_2^- (π^*) charge transfer (ILCT) and $L_{IS}^{\bullet-}$ to d-orbitals of vanadium charge transfer (LMCT), which are responsible for the absorption of these species at 400−600 nm.

Table 1. Crystallographic Data of 1•3/2MeOH and 3•1/2L^{Me}_{AP}

formula	$C_{24}H_{18}N_3O_3V$•3/2MeOH	$C_{44}H_{34}N_8O_6V_2$•L^{Me}_{AP}
fw	495.42	995.82
crystal color	dark brown	dark brown
crystal system	monoclinic	triclinic
space group	$P2_1/c$	$P1$
a (Å)	8.059(1)	13.073(1)
b (Å)	15.123(1)	13.084(1)
c (Å)	19.229(1)	14.355(2)
α (deg)		97.372(2)
β (deg)	90.901(1)	97.313(2)
γ (deg)		111.245(1)
V (Å^3)	2343.70(7)	2229.4(4)
Z	4	2
T (K)	296(2)	293(2)
calcd (g cm^{-3})	1.404	1.483
unique reflections	4076	8711
refection [$I > 2\sigma(I)$]	3751	7011
λ (Å), μ (mm^{-1})	0.71073/0.463	0.71073/0.486
F(000)	1028	1028
R1[a] [$I > 2\sigma(I)$)]/ GoF [b]	0.0440/1.179	0.0534/1.014
R1[a] (all data)	0.0479	0.0658
wR2[c] ($I > 2\sigma$ (I))	0.1075	0.1487
no. of parameters/restr.	320/0	647/0
residual density (eÅ^{-3})	0.560	0.799

[a] $R1 = \Sigma||F_o| - |F_c||/\Sigma|F_o|$. [b] $GooF = \{\Sigma[w(F_o^2 - F_c^2)^2]/(n-p)\}^{1/2}$. [c] $wR2 = \{\Sigma[w(F_o^2 - F_c^2)^2]/\Sigma[w(F_o^2)^2]\}^{1/2}$ where $w = 1/[\sigma^2(F_o^2) + (aP)^2 + bP]$, $P = (F_o^2 + 2F_c^2)/3$.

3. RESULTS AND DISCUSSION

3.1. Syntheses and Characterization. The diamagnetic oxidovanadium(IV) complexes, $(L^{-})(VO^{2+})(L^{R}_{IS}{}^{\bullet-})$ (R = H, Me; L = L_1 and L_2 are two tridentate NNO-donor ligands), incorporating iminobenzosemiquinonate anion radicals ($L^{R}_{IS}{}^{\bullet-}$) isolated in this work, are listed in Chart 2.

The tridentate diimine ligand L_1H has not been preisolated (L_1H = 2-[(phenylpyridin-2-yl-methylene)amino]phenol). But the complex of L_1, **1**•3/2MeOH, has been isolated in good yield from a single step reaction of 2-benzoyl pyridine, 2-aminophenol and $VO(acac)_2$ in a mixture of solvents using air as an oxidizing agent. Compounds **2** and **3**•1/2 L^{Me}_{AP} have been synthesized by reacting L_2H (L_2H = 1-(2-pyridylazo)-2-naphthol), $VO(acac)_2$ and corresponding aminophenol (L^{R}_{AP}) in methanol and dichloromethane under air. N−H stretching vibrations of **1**•3/2MeOH, **2** and **3**•1/2 L^{Me}_{AP} complexes resonate at 3210, 3206, and 3198 cm^{-1} and V═O stretching vibrations appear respectively at 946, 952, and 937 cm^{-1}.

Compounds **1**•3/2MeOH, **2**, and **3**•1/2 L^{Me}_{AP} absorb strongly in the visible region (Figure 1). The absorptions data are summarized in Table 2. In dichloromethane, **1**•3/2MeOH is very weakly luminescent, but it is moderately luminescent in frozen dichloromethane−toluene glass at 77 K (λ_{ext}, 333 nm; λ_{em}, 522 and 553 nm). The luminescence feature is very similar to that of the brightly luminescent (L_1^{-})ZnX species in solution at room temperature.[22] DFT calculations on (L_1^{-})ZnX have assigned the $\pi_{diimine} \rightarrow \pi_{diimine}{}^{*}$ transitions as the origin of luminescence. Thus, compound **1**•3/2MeOH is luminescent in solution because of the coordinated L_1^{-} chromophore.

Other than the strong absorption band at around 445 nm, complexes **2** and **3**•1/2 L^{Me}_{AP} show a strong absorption band with the maximum at around 585 nm. TD DFT calculations on the singlet state of **2** have assigned the intra-ligand charge transfer (ILCT) and ligand-to-metal charge transfer (LMCT) as the origins of absorption of these species in the visible region (Section 3.3).

Chart 2. Isolated $(L^{-})(VO^{2+})(L^{R}_{IS}{}^{\bullet-})$ Complexes

$(L_1^{-})(VO^{2+})(L^{H}_{IS}{}^{\bullet-})$·3/2MeOH — **1**·3/2MeOH

$(L_2^{-})(VO^{2+})(L^{H}_{IS}{}^{\bullet-})$ — **2**

$(L_2^{-})(VO^{2+})(L^{Me}_{IS}{}^{\bullet-})$·1/2$L^{Me}_{AP}$ — **3**·1/2L^{Me}_{AP}

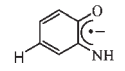

= $L^{H}_{IS}{}^{\bullet-}$

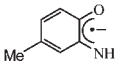

= $L^{Me}_{IS}{}^{\bullet-}$

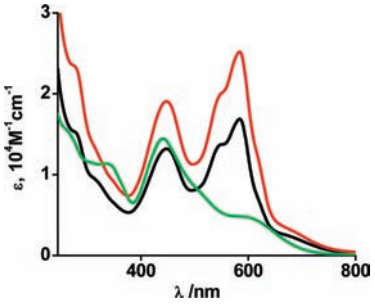

Figure 1. Electronic spectra of **1**•3/2 MeOH in MeOH (green), **2** (red), and **3**•1/2 L^{Me}_{AP} (black) in dichloromethane.

3.2. X-ray Structures. *1•3/2MeOH.* The geometry of **1**•3/2MeOH has been confirmed by the single-crystal X-ray structure determination. It crystallizes in the $P2_1/c$ space group. An ORTEP plot of the molecule and the atom-labeling scheme are illustrated in Figure 2. Table 3 summarizes the significant bond parameters. The meridionaly coordinated tridentate monoanionic diimine ligand (L_1^{-}), excluding the pendent phenyl ring, is planar with a mean deviation of 0.05 Å. With respect to this plane, the vanadium atom is about 0.3 Å displaced toward the terminal oxido atom. The *o*-aminophenolato ligand coordinates the vanadium ion with the phenolato oxygen *trans* to the terminal oxido bond.

The bond parameters of the octahedral coordination sphere are informative to assign the VO^{n+} state. The terminal V═O bond is not expected to depend much on the $V^{IV}O$ or $V^{V}O$ state. In **1**•3/2MeOH, the V1−O1 length is 1.610(2) Å. The length is longer than those reported in the mononuclear $V^{V}O$ species with similar types of coordination environments.[8,23,24,26] The V(1)−O(1) length rather compares very well with the average V^{IV}═O length, 1.600 Å, calculated from 1000 structures deposited in CCDC.[25] The length of V(1)−O(3), a $V-O_{phenolato}$ bond *cis* to the V═O, is significant as it sharply depends on the VO^{2+} or VO^{3+} chromophore. It is reported that the average $V-O_{phenolato}$ distance is 1.81 and 1.91 Å for oxidovanadium(V) and oxidovanadium(IV), respectively.[26] So far, the shortest $V^{IV}-O_{phenolato}$ distance is 1.887(4) Å, reported in a weakly diffracting oxidovanadium(IV) complex of 1-(2-hydroxybenzamido)-2-(2-pyridinecarboxamido)benz ligand.[26d] In **1**•3/2MeOH, the V(1)−O(3) length, 1.939(2) Å, is comparable with those in $V^{IV}-O_{phenolato}$ bonds *cis* to the V═O bond, prompting the presence of $V^{IV}O$. This length trend of $V^{V/IV}-O_{phenolato}$ bonds *cis* to a V═O bond has been authenticated in many other mononuclear[8−10,23,24] and binuclear mixed valence species.[23a]

The bond parameters of the coordinated redox non-innocent *o*-aminophenolate are important to assign its oxidation level and the oxidation state of the vanadium ion. In **1**•3/2MeOH, it can exist either as a diamagnetic bidentate dianionic *o*-amidophenolato ligand ($L^{H}_{AP}{}^{2-}$) coordinated to a diamagnetic VO^{3+} core or

Table 2. Electronic Spectra of 1•3/2 MeOH, 2, and 3•1/2L^{Me}_{AP} and Electrochemically Generated 3^{+} and 3^{-} Ions in Dichloromethane at 20°C

complexes	λ_{max} (nm) (ε, 10^4 M^{-1} cm^{-1})
1•3/2 MeOH	604 (0.5), 507(0.8), 442 (1.4), 340 (1.1), 264 (1.5)
2	685(0.3), 620(1.2), 583(2.5), 544(1.9), 447(1.9),316(1.3) 277(2.3)
3•1/2 L^{Me}_{AP}	682(0.2), 621(0.66), 585(1.7), 545(1.3) 447(1.3), 316(0.9), 278(1.5)
3^{-}	688(0.9), 625(1.1), 581(1.7), 546(1.6) 492(1.5),446(1.9), 313(1.7), 281(2.1)
3^{+}	681(0.6), 620(0.9), 577(1.2), 543(1.1) 495(1.3),460(1.5),338(0.9), 306(1.2), 286(1.2)

dx.doi.org/10.1021/ic102296p |*Inorg. Chem.* 2011, 50, 2488–2500

Table 3. Selected Experimental Bond Lengths (Å) and Angles (deg) of 1•3/2MeOH and Calculated Parameters of 1, 1^+ and 1^-, using B3LYP, B3PW91, and PBE1PBE Functionals

		calcd					
	exp	1				1^+	1^-
	1•3/2 MeOH	BS (1,1) $M_s = 0^a$	BS (1,1) $M_s = 0^b$	BS (1,1) $M_s = 0^c$	$M_s = 1^a$	$M_s = 1/2^a$	$M_s = 1/2^a$
V(1)−O(1)	1.610(2)	1.600	1.594	1.588	1.599	1.582	1.606
V(1)−O(2)	2.131(2)	2.116	2.096	2.090	2.192	2.323	2.158
V(1)−O(3)	1.940(2)	1.920	1.910	1.903	1.938	1.875	1.913
V(1)−N(1)	1.908(2)	1.888	1.877	1.868	2.063	2.011	1.907
V(1)−N(2)	2.110(2)	2.128	2.110	2.104	2.174	2.124	2.112
V(1)−N(3)	2.120(2)	2.174	2.159	2.148	2.144	2.119	2.090
O(2)−C(6)	1.312(3)	1.299	1.297	1.295	1.281	1.248	1.295
N(1)−C(1)	1.362(3)	1.367	1.365	1.365	1.330	1.313	1.370
O(3)−C(7)	1.325(3)	1.309	1.305	1.303	1.306	1.363	1.353
C(1)−C(2)	1.399(4)	1.408	1.405	1.402	1.424	1.434	1.404
C(2)−C(3)	1.368(4)	1.387	1.387	1.385	1.378	1.364	1.395
C(3)−C(4)	1.395(5)	1.412	1.408	1.407	1.423	1.450	1.407
C(4)−C(5)	1.366(4)	1.388	1.387	1.386	1.380	1.362	1.393
C(5)−C(6)	1.391(4)	1.415	1.411	1.409	1.423	1.444	1.416
C(6)−C(1)	1.419(4)	1.435	1.429	1.428	1.472	1.499	1.437
N(3)−C(13)	1.297(3)	1.302	1.305	1.296	1.303	1.305	1.350
O(1)−V(1)−O(2)	171.06(9)	166.63	166.44	166.48	166.09	165.45	166.13
O(1)−V(1)−N(1)	95.51(10)	94.26	93.83	93.95	98.82	95.36	92.23
O(2)−V(1)−N(1)	76.92(8)	76.97	77.16	77.30	75.08	72.79	75.56
O(1)−V(1)−O(3)	101.11(9)	102.31	102.07	103.19	103.63	105.46	100.50

[a] B3LYP. [b] B3PW91. [c] PBE1PBE.

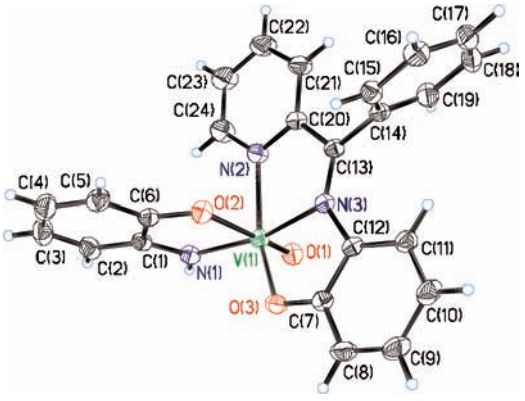

Figure 2. ORTEP plot of **1**•3/2MeOH (40% thermal ellipsoids; solvent molecules are omitted for clarity).

as a one electron paramagnetic bidentate iminobenzosemiquinonate anion radical ($L^{H}_{IS}{}^{\bullet-}$) coordinated to the paramagnetic VO^{2+} core (Figure 3). The bond parameters of this NO chelate show comparatively shorter O(2)−C(6) and C(1)−N(1) distances and a quinoidal distortion of the aromatic ring with the adjacent long−short−long−short C−C bonds: C(1)−C(2), 1.399(4); C(2)−C(3), 1.368(4); C(3)−C(4), 1.412(4); and C(4)−C(5), 1.366(4) Å as shown in panel (B) of Figure 3. The features correlate satisfactorily to the bond parameters of $L^{H}_{IS}{}^{\bullet-}$ coordinated to a transition metal ion, established precisely by Wieghardt et al.[27] and other groups.[28] This trend of bond parameters does not support the type I coordination of $L^{H}_{AP}{}^{2-}$ as shown in panel (a) of Figure 3. In **1**•3/2MeOH, $L^{H}_{IS}{}^{\bullet-}$ thus

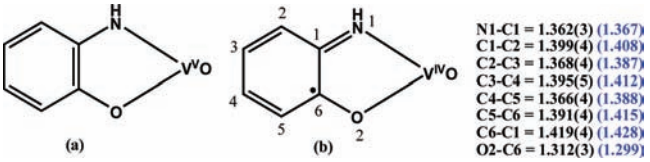

Figure 3. (a) *o*-Amidophenolato dianion ($L^{H}_{AP}{}^{2-}$) coordinated to VO^{3+} (type I coordination). (b) Iminobenzosemiquinonate anion radical ($L^{H}_{IS}{}^{\bullet-}$) coordinated to a VO^{2+} ion (type III coordination). Experimental and calculated (in parentheses) bond lengths (Å) of the fragment, respectively, in **1**•3/2MeOH and BS (1,1) $M_s = 0$ state of **1**.

coordinates to a VO^{2+} core (type III, Chart 1) as shown in panel (b) of Figure 3.

The V(1)−O(2) bond, 2.131(2) Å, is longer compared to the V(1)−O(3) bond because of the *trans* influence of the V=O bond. It has been observed that the $V-O_{phenolato}$ bond *trans* to V=O is ≥0.20 Å longer than the $V-O_{phenolato}$ bond *cis* to V=O in the same coordination sphere. This lengthening parameter has been extracted from the reported oxidovanadium(V) complexes of catecholates.[8a−d,9] Subtracting the lengthening (0.20 Å) due to *trans* influence, the V(1)−O(2) bond distance, 1.931 Å, in **1**•3/2MeOH is consistent with the $V^{IV}-O_{phenolato}$ description.[8c,26c] It is noted that in **1**•3/2MeOH, the V(1)−N(1) bond, 1.908(2) Å, is shorter than the reported $V^{V}-N_{amidophenolato}$ bond, ≥1.946(3) (Å), *cis* to a V=O bond.[10a] It signifies the stronger affinity of OV^{IV} toward the iminobenzosemiquinonate anion radical ($L^{H}_{IS}{}^{\bullet-}$) than that of the *o*-amidophenolato dianion ($L^{H}_{AP}{}^{2-}$). The result correlates well to the higher affinity of OV^{IV} to the *p*-benzosemiquinonate anion radical than to phenolato oxygen,

dx.doi.org/10.1021/ic102296p |*Inorg. Chem.* 2011, 50, 2488–2500

revealing a comparatively shorter $V^{IV}-O_{semiquinonate}$ length (1.880(2)−1.937(2) Å).[9] However, in the literature, no structure of $L^{H}{}_{IS}{}^{\bullet-}$ coordinated to $VO^{2+/3+}$ chromophore has been reported so far to be compared.

3•1/2L$^{Me}{}_{AP}$. The molecular geometries of **2** and **3**•1/2 $L^{Me}{}_{AP}$ in crystals have been confirmed by single-crystal X-ray structure determination of **3**•1/2 $L^{Me}{}_{AP}$. The complex **3** crystallizes with half of an *o*-amino-*p*-methylphenol molecule (1/2 $L^{Me}{}_{AP}$), which is severely disordered in the lattice. It crystallizes in the *P*1 space group. An ORTEP plot of the molecule and the atom-labeling scheme are illustrated in Figure 4. Selected bond parameters are listed in Table 4. The geometrical features and bond parameters of **3**•1/2 $L^{Me}{}_{AP}$ are similar to those found in **1**•3/2MeOH. The meridionally coordinated tridentate monoanionic azo ligand (L_2^-) is completely planar with a mean deviation of 0.04 Å, and the vanadium atom is displaced toward the terminal oxido atom only by 0.08 Å.

The bond length trend in **3**•1/2 $L^{Me}{}_{AP}$ strongly supports the $V^{IV}O$ description as in **1**•3/2MeOH. The V(1)−O(1) length is 1.621(2) Å. The V(1)−O(3), a $V-O_{phenolato}$ bond *cis* to the V═O, length is 1.984(2) Å, even longer than those found in **1**•3/2MeOH and other reported $V^{IV}O$ phenolato species.[8−10,23,24,26] The V(1)−O(2) bond, 2.083(2) Å, is longer due to the *trans* influence of the V═O bond as observed in **1**•3/2MeOH. Comparatively shorter O(2)−C6 and C(1)−N(1) distances and a quinoidal distortion of the aromatic phenyl ring with the adjacent long−short−long−short C−C bonds: C(1)−C(2), 1.409(4); C(2)−C(3), 1.373(4); C(3)−C(4), 1.414(4); and C(4)−C(5), 1.375(4) Å as in Figure 5, correlate well to the coordinated bidentate *o*-imino-*p*-methylbenzosemiquinonate anion radical ($L^{Me}{}_{IS}{}^{\bullet-}$) as shown in panel (b) of Figure 5. The bond length trends do not favor coordination of $L^{Me}{}_{AP}{}^{2-}$ to VO^{3+} as shown in panel (a) of Figure 5. Thus, in **3**•1/2 $L^{Me}{}_{AP}$,

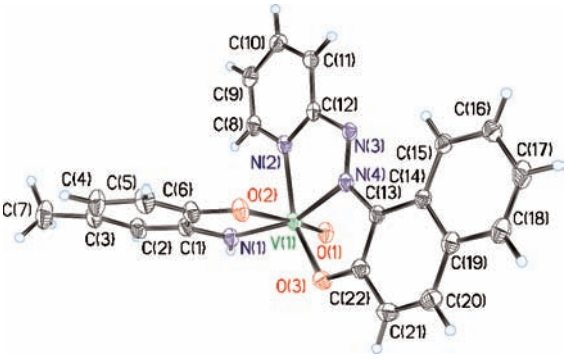

Figure 4. ORTEP plot of **3**•1/2 $L^{Me}{}_{AP}$ (40% thermal ellipsoids, $L^{Me}{}_{AP}$ molecule is omitted for clarity).

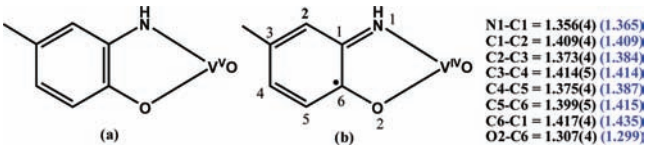

Figure 5. (a) *o*-Amido-p-methylphenolato dianion ($L^{R}{}_{AP}{}^{2-}$) coordinated to VO^{3+} (type I coordination). (b) *o*-Imino-*p*-methylbenzosemiquinonate anion radical ($L^{Me}{}_{IS}{}^{\bullet-}$) coordinated to VO^{2+} (type III coordination). Experimental and calculated (in parentheses) bond lengths (Å) of the fragment, respectively, in **3**•1/2 $L^{Me}{}_{AP}$ and BS (1,1) $M_s = 0$ state of **2**.

Table 4. Selected Experimental Bond lengths (Å) and Angles (deg) of 3•1/2L$^{Me}{}_{AP}$ and Calculated Parameters of 2, 2^+, and 2^- using UB3LYP Functional

		calcd			
	exp	**2**		2^+	2^-
	3•1/2 $L^{Me}{}_{AP}$	BS (1,1) $M_s = 0$	$M_s = 1$	$M_s = 1/2$	$M_s = 1/2$
V(1)−O(1)	1.621(2)	1.598	1.596	1.579	1.605
V(1)−O(2)	2.083(2)	2.108	2.226	2.323	2.144
V(1)−O(3)	1.984(2)	1.976	1.993	1.925	1.929
V(1)−N(1)	1.921(2)	1.891	2.071	2.014	1.908
V(1)−N(2)	2.081(3)	2.109	2.141	2.100	2.097
V(1)−N(4)	2.102(2)	2.142	2.091	2.095	2.089
O(2)−C(6)	1.307(4)	1.299	1.280	1.246	1.295
N(1)−C(1)	1.356(4)	1.365	1.333	1.312	1.370
O(3)−C(22)	1.300(4)	1.285	1.286	1.305	1.314
C(1)−C(2)	1.409(4)	1.409	1.425	1.434	1.404
C(2)−C(3)	1.373(4)	1.384	1.377	1.364	1.394
C(3)−C(4)	1.414(5)	1.414	1.425	1.452	1.407
C(4)−C(5)	1.375(4)	1.387	1.379	1.361	1.393
C(5)−C(6)	1.399(5)	1.415	1.425	1.445	1.415
C(6)−C(1)	1.417(4)	1.435	1.471	1.501	1.436
N(3)−N(4)	1.285(3)	1.291	1.292	1.292	1.332
O(1)−V(1)−O(2)	171.70(9)	168.99	170.69	167.04	166.36
O(1)−V(1)−N(1)	94.82(11)	93.89	98.33	95.49	91.91
O(2)−V(1)−N(1)	76.91(9)	76.83	99.18	72.71	75.66
O(1)−V(1)−O(3)	97.60(11)	100.27	102.47	103.66	100.43

dx.doi.org/10.1021/ic102296p |*Inorg. Chem.* 2011, 50, 2488–2500

$L^{Me}{}_{IS}{}^{\bullet-}$ coordinates to a VO^{2+} core confirming the existence of type III coordination as in **1**•3/2MeOH.

3.3. Electrochemical Activities and Spectroelectrochemistry. The electrochemical activities of **1**•3/2MeOH, **2**, and **3**•1/2 $L^{Me}{}_{AP}$ to assess the stabilities of the corresponding one electron oxidized and reduced species in solutions have been studied at 20 °C by cyclic voltammetry in CH_2Cl_2 containing 0.2 M tetrabutyl ammonium hexafluorophosphate as supporting electrolyte. All the experiments were performed with different scan rates. The reduction potential data have been referenced versus ferrocenium/ferrocene, Fc^+/Fc, couple and are summarized in Table 5. The compound **1**•3/2MeOH exhibits one electron transfer waves with the peak at +0.32 V due to $\mathbf{1}^+/\mathbf{1}$ and another two electron transfer wave with the peak at −1.36 V due to $\mathbf{1}/\mathbf{1}^{2-}$ couples. The voltammogram is given in panel (a) of Figure 6, which shows that both couples are irreversible in all scan rates, showing both the oxidized and reduced species are unstable in solutions. The electron transfer events in **2** are also irreversible (Figure 6b) with a quasi-reversible peak at −1.04 V. The electron transfer events are more reversible in **3**•1/2 $L^{Me}{}_{AP}$ (Figure 6c),

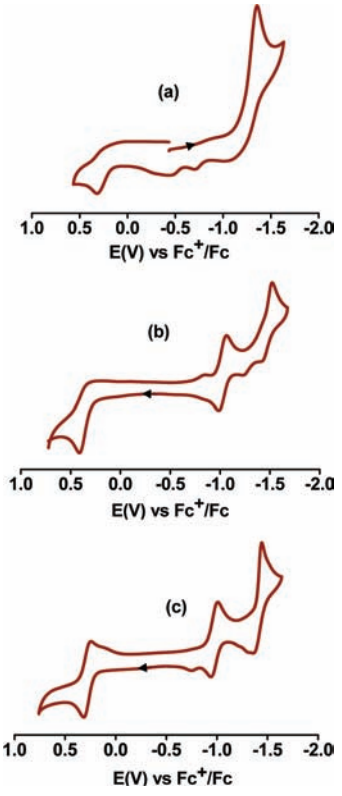

Figure 6. Cyclic voltammograms of (a) **1**•3/2MeOH, (b) **2**, and (c) **3**•1/2 $L^{Me}{}_{AP}$ in dichloromethane at 20 °C. Conditions: 0.10 M $[N(n\text{-}Bu)_4]PF_6$ supporting electrolyte; scan rate, 100 mv s^{-1}; glassy carbon working electrode.

and reduction occurs by transfer of consecutive two electrons. However, the one electron oxidized ($S = 1/2$) and reduced species ($S = 1/2$) are unstable in solutions, and we failed to record reproducible EPR spectra of them even at 77 K.

The origin of the absorption spectrum of **2** with singlet spin state has been investigated by TD-DFT calculations. Analyses of transition types and excitation energies of the transitions with oscillator strength greater than 0.04 at 400−600 nm have shown that two types of transitions are responsible for the absorptions at 600−400 nm. These are iminobenzosemiquinonate anion radical ($L^{H}{}_{IS}{}^{\bullet-}$) to the unoccupied d-orbital of vanadium charge transfer (LMCT) and π to $\pi_{azo}{}^*$ of $L_2{}^-$ charge transfer (ILCT). The low-energy absorption bands at 580−550 nm of **2** and **3**•1/2 $L^{Me}{}_{AP}$ are weaker in **1**•3/2MeOH. The origin of this strong absorption band in **2** and **3**•1/2 $L^{Me}{}_{AP}$ has been assigned to transition to $\pi_{azo}{}^*$ of $L_2{}^-$ ligand (ILCT). Electronic structures of $\mathbf{1}^-$, $\mathbf{2}^-$ and $\mathbf{1}^+$, $\mathbf{2}^+$ ions have been predicted as $[(L_1{}^{\bullet 2-})(VO^{3+})(L^{H}{}_{AP}{}^{2-})]^-$ ($\mathbf{1}^-$), $[(L_2{}^{\bullet 2-})(VO^{3+})(L^{H}{}_{AP}{}^{2-})]^-$ ($\mathbf{2}^-$), and $[(L_1{}^-)(VO^{2+})(L^{H}{}_{IQ})]^+$($\mathbf{1}^+$), $[(L_2{}^-)(VO^{2+})(L^{H}{}_{IQ})]^+$ ($\mathbf{2}^+$) by DFT calculations (Section 3.4). Calculations show that oxidation occurs at $L^{R}{}_{IS}{}^{\bullet-}$ rendering coordinated *o*-iminiquinone ($L^{R}{}_{IQ}$) unaffecting the tridentate NNO-donor ligands ($L_1{}^-/L_2{}^-$) in $\mathbf{1}^+$ and $\mathbf{2}^+$, while in $\mathbf{1}^-$ and $\mathbf{2}^-$, reduction of $L^{R}{}_{IS}{}^{\bullet-}$ to $L^{R}{}_{AP}{}^{2-}$ concomitantly transforms uncoupled VO^{2+} to VO^{3+} ions reducing $L_1{}^-/L_2{}^-$ to coordinated diimine/azo anion radicals ($L_1{}^{2-\bullet}/L_2{}^{2-\bullet}$). Changes of absorption spectra upon one electron reduction or oxidation of **3**•1/2 $L^{Me}{}_{AP}$ in dichloromethane solvent at 298 K have been monitored by spectroelectrochemistry experiments (Figure 7). Panel (a) of Figure 7 shows the conversion of **3** to $\mathbf{3}^+$ with several isosbestic points changing the absorption features at 400−600 nm. It occurs by lowering the intensity of the band maxima at 583 nm and shifting the absorption band maxima at 447 to 460 and 495 nm. These features corroborate well with the change of the electronic structures of the $L^{R}{}_{IS}{}^{\bullet-}$ ligand in $\mathbf{3}^+$. But conversion of **3** to $\mathbf{3}^-$ does not show any significant change of spectral features (Figure 7b) of **3** except the intensity, correlating well with the same electronic structures of the anion radical ligand ($L^{R}{}_{IS}{}^{\bullet-}$) in $\mathbf{3}^-$.

In all complexes, irrespective of the tridentate ligands, reduction processes occuring by two electron transfer generating $\mathbf{1}^{2-}$, $\mathbf{2}^{2-}$, and $\mathbf{3}^{2-}$ may be due to the easy formation of coupled VO^{2+}−diimine/azo anion radical complexes, $[(L^{\bullet 2-})(VO^{2+})(L^{R}{}_{AP}{}^{2-})]^{2-}$ from monoreduced uncoupled diimine/azo anion radical species, $[(L^{\bullet 2-})(VO^{3+})(L^{R}{}_{AP}{}^{2-})]^-$.

3.4. BS-DFT Calculations. In conjunction with the experimental efforts, the electronic structures of **1**•3/2MeOH, **2**, and **3**•1/2 $L^{Me}{}_{AP}$ to correlate bond parameters and spectral features have been elucidated by density functional theory (DFT) calculations on **1** and **2**, using B3LYP, B3PW91, and PBE1PBE functionals. For, comparison the geometry of a soft complex, $(L_1{}^-)(VO^{3+})(gly^{2-})$ (**4**), incorporating a redox innocent ethylene glycolate dianion (gly^{2-}) and acting as a model compound of VO^{3+} (type I coordination, Chart 1) has been optimized to establish the trend of bond parameters (Scheme 2). DFT

Table 5. Redox Potential of 1•3/2MeOH, 2, and 3•1/2$L^{Me}{}_{AP}$ Determined by Cyclic Voltammetry at 20°C in Dichloromethane

complexes	$E_{1/2}$ (V) (ΔE, mV) (+1/0)	$E_{1/2}$ (V) (ΔE^a, mV) (0/−1)	$E_{1/2}$ (V) (ΔE, mV) (−1/−2)
1•3/2MeOH	+0.32[b]	−1.36[c]	
2	+0.41[b]	−1.04(72)	−1.48(100)
3•1/2 $L^{Me}{}_{AP}$	+0.28(65)	−0.98(60)	−1.41(80)

[a] Peak-to-peak separation. [b] Anodic peak. [c] Cathodic peak.

dx.doi.org/10.1021/ic102296p |*Inorg. Chem.* 2011, 50, 2488–2500

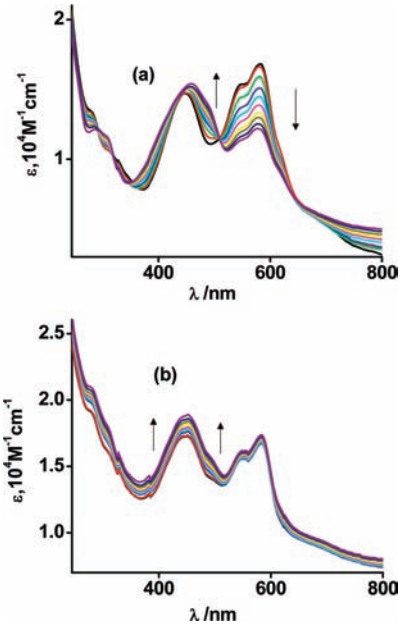

Figure 7. Spectroelectrochemistry of **3**•1/2 L^{Me}_{AP} showing the electronic spectra of electrochemically generated (a) 3^{+} and (b) 3^{-} in dichloromethane at 20 °C.

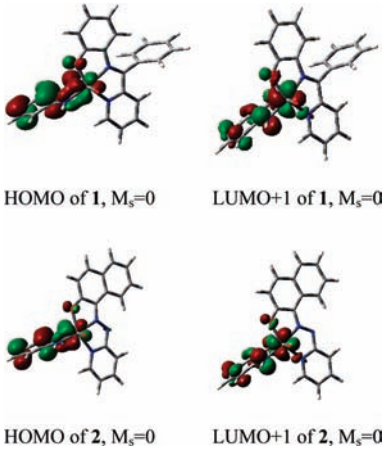

Figure 8. Closed shell singlet (CSS) solutions of **1** and **2**.

calculations are to confirm the electronic structures of **1**−**3**, and the question is which type of core species **1**−**3** incorporate, VO^{3+} (type I) or VO^{2+} (type III), as shown in Figures 3 and 5.

Initially, the geometries of **1** and **2** have been optimized using singlet spin state at the RB3LYP, RB3PW91, or PBE1PBE level of the theory. Molecular orbital analyses of these restricted solutions of **1** and **2** have shown that in both cases HOMOs are composed of vanadium and aminophenol ligand as shown in Figure 8. The contribution of the vanadium d-orbital to HOMOs is of concern in elucidating the electronic structures of **1** and **2**. Thus, the stabilities of the singlet self-consistent field (SCF) solutions of **1** and **2** were tested. Surprisingly, it is observed that the closed shell singlet (CSS) solutions of these oxidovanadium complexes are unstable with respect to triplet perturbations as the lowest Hessian eigenvalues are negative for all these species. For **1**, it is −0.0211with B3LYP, −0.01700 with B3PW91, and −0.018 with PBE1PBE functionals due to HOMO to

Scheme 2. Compound 4 (Type I Coordination) and the HOMO

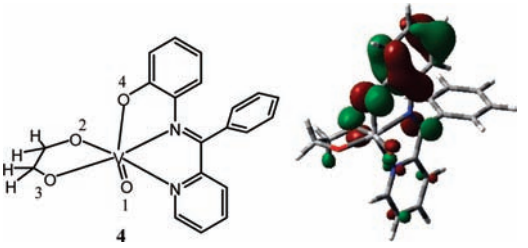

LUMO+1 excitations. Both these orbitals are composed of vanadium metal and *o*-aminophenolate ligand. But the major contribution of the HOMO is *o*-aminophenol ligand, while the major contribution of the LUMO+1 is the vanadium d-orbital (Figure 8).

Similar features have been observed in **2** also, and the lowest Hessian eigenvalue here is −0.0224 with B3LYP functional again due to HOMO to metal LUMO+1 excitation. These negative lowest eigenvalues of excitations of these species contradict the closed shell singlet (CSS) as a stable ground state. It implies that either the lowest energy wave function is a singlet diradical instead of a closed shell singlet and requires an unrestricted broken symmetry (BS) solution for proper descriptions or the triplet state (S = 1) is energetically more favorable than the lowest lying singlet state. Stability analyses followed by reoptimization of the singlet states using the BS method leads to solutions with a large amount of diradical character in **1** and **2** (**1** = 71% with B3PLYP, 68% with B3PW91, and 74% with PBE1PBE functionals; **2** = 73% with B3PLYP functional), depicting the $L^{H}_{IS}{}^{\bullet-}$ coordinated to the one electron paramagnetic oxidovanadium(IV) ion confirming type III coordination in **1** and **2** as shown in Figures 3 and 5. To define, the system is divided into two fragment,s and the notation BS (1,1) refers to a broken symmetry state with 1 unpaired spin-up electron on a $L^{H}_{IS}{}^{\bullet-}$ fragment and 1 unpaired spin-down electron essentially localized on a VO^{2+} core. Bond parameters of the BS (1,1) M_s = 0 solutions of **1** and **2** are similar to those found in CSS solutions, but the BS (1,1) M_s = 0 solutions are stable under the perturbations considered. The geometries of **1** and **2** with triplet states (S = 1, type III coordination) have also been optimized for comparison using similar basis sets for vanadium ion and other nonmetal atoms. It has been established that among the CSS, BS (1,1) Ms = 0 and triplet (S = 1) solutions, the unrestricted BS (1,1) Ms = 0 solutions of **1** and **2** with B3LYP, B3PW91, and PBE1PBE functionals, corroborating singlet diradicals, have the lowest ground state energy.

On the contrary, the CSS solution of the model soft compound **4** incorporating a redox innocent gly^{2-} ligand (Scheme 2) under similar coordination sphere and calculation parameters is stable. Unlike **1**or **2**, HOMO of **4** does not have any vanadium contribution (Scheme 2). The wave function has no instability due to triplet perturbations. It prompts the coordination of the dianionic ligand to the oxidovanadium(V) ion in **4** (type I coordination). Calculated bond distances of this oxidovanadium(V) complex incorporating dianionic gly^{2-} are different from those of oxidovanadium(IV) species (**1** and **2**), incorporating the iminobenzosemiquinonate anion radical. Selected calculated distances are listed in Table 6. The

dx.doi.org/10.1021/ic102296p |*Inorg. Chem.* 2011, 50, 2488–2500

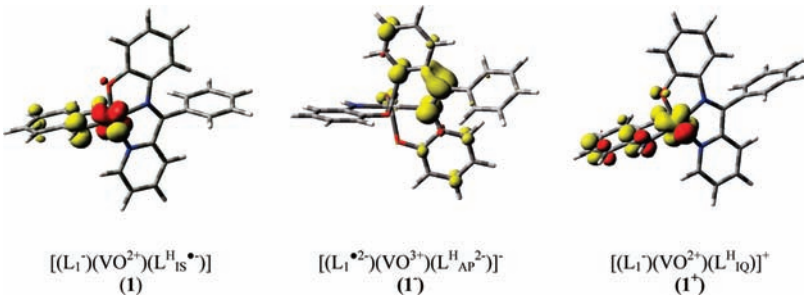

Figure 9. Spin density plot of **1**, $\mathbf{1}^-$, and $\mathbf{1}^+$ (yellow, α spin; red, β spin) and values from Mulliken spin population analyses (spin density, **1**: V, −0.71, N1, 0.26, O2, 0.10, O1, 0.10, C4, 0.10, C6, 0.08. $\mathbf{1}^-$: N2, 0.14, N3, 0.22, C3, 0.15, C13, 0.22. $\mathbf{1}^+$:V, 0.83).

bond length trend is noteworthy. The calculated V═O distances in **1**, **2**, and **4** are comparable as observed in VO^{2+} and VO^{3+} complexes experimentally. But in **4**, the calculated V−O(phenolato), V−O(4), length *cis* to the V═O bond is only 1.870 Å, which is 1.940 (calcd, 1.920 Å for **1**) and 1.984 Å (calcd, 1.976 Å for **2**), respectively, in **1**•3/2MeOH and **3**•1/2 $L^{Me}{}_{AP}$ complexes. This proves that the V−O(phenolato) bond length (*cis* to V═O) remarkably depends on the $VO^{2+/3+}$ states as observed experimentally, too.[26] Another significant outcome of the calculations on **4** is that the V−O(2) length is longer than the V−O(3) length by ∼0.16 Å because of the *trans* influence of the V═O bond, which has already been noted in experimental V−O(2) lengths of **1**•3/2MeOH and **3**•1/2 $L^{Me}{}_{AP}$ complexes.

Although, one electron oxidized cations and one electron reduced anions of **1** and **2** have not been successfully isolated, the geometries of these species have been optimized to investigate the trend of change of bond parameters of the coordinated *o*-aminophenolate ligand. The calculated lengths are listed in Tables 3 and 4. The electron transfer states of these species are shown in Scheme 1. The trend of lengths of the vanadium sphere as well as the coordinated ligand of neutral, oxidized, and reduced species is worthy to establish the electronic structure of **1**−**3** species unambiguously.

*$(L_1{}^-)(VO^{2+})(L^H{}_{IS}{}^{\bullet-})$ (**1**) (Type III Coordination).* With the B3LYP functional, the BS (1,1) M_s = 0 solution (type III coordination) of **1** is stabilized by 6.3 and 20.2 KJ/mol compared to the CSS (type I coordination) and the triplet (S = 1, type III coordination) solutions, respectively. The bond parameters of the BS (1,1) M_s = 0 (with B3LYP, B3PW91, and PBE1PBE functionals) and open shell triplet (S = 1) solutions are listed in Table 3 for comparison. The calculated bond parameters of the triplet solution, particularly V(1)−O(2), V(1)−N(1), V(1)−N(2), O(2)−C(6), and C(1)−N(1), are significantly different from the experimental lengths. Excellent agreement of the calculated bond parameters of BS (1,1) M_s = 0 state of **1** with those found in the single-crystal X-ray structure of **1**•3/2MeOH favor the spin-coupled type III coordination as shown in Figure 3. Mulliken spin density distributions are depicted in Figure 9, which affirm the d^1 electronic configuration of the oxidovanadium ion (beta spin). The alpha spin is delocalized over the coordinated bidentate $L^H{}_{IS}{}^{\bullet-}$ ligand with the maximum at the $N_{iminosemiquinonate}$ (N1) atom. Both V(1)−N(1) and V(1)−O(2) lengths of the $L^H{}_{IS}{}^{\bullet-}$ chelate have been reproduced well. Two calculated V(1)−$O_{phenolato}$ lengths, V(1)−O(2) (2.116 Å) and V(1)−O(3) (1.920 Å), are significantly different as observed experimentally. Because of the *trans* influence of the V═O bond, the V(1)−O(2) length is higher than expected and that has also been established by calculation on the model compound **4** (Scheme 2, Table 6). The calculated C(1)−N(1) and O(2)−C(6) lengths, respectively, 1.367 and 1.299 Å, are characteristic for an iminobenzosemiquinonate anion radical ($L^H{}_{IS}{}^{\bullet-}$). The calculation has identified a quinoidal distortion of the aromatic phenyl ring with the adjacent long−short−long−short C−C bonds (Figure 3) that has also been observed in the experimental lengths of **1**•3/2MeOH. Thus, compound **1** has been described as a vanadyl species of type $(L_1{}^-)(VO^{2+})(L^H{}_{IS}{}^{\bullet-})$ as shown in panel (b) of Figure 3.

Table 6. Selected Calculated Bond Lengths (Å) of 4 (Type I Coordination)

V−O(1)	1.611
V−O(2)	1.962
V−O(3)	1.804
V−O(4)	1.870
$V-N_{py}$	2.167
$V-N_{imine}$	2.209
O4−C3	1.320
−N=CPh−	1.297

*$[(L_1{}^-)(VO^{2+})(L^H{}_{IQ})]^+$ (**1**$^+$) (Type V Coordination).* The spin density distribution (Figure 9) explains the $[(L_1{}^-(VO^{2+})(L^H{}_{IQ})]^+$ description of the $\mathbf{1}^+$ cation ($L^H{}_{IQ}$ = iminobenzoquinone). This observation strongly supports the presence of a VO^{2+} ion and a $L^H{}_{IS}{}^{\bullet-}$ anion radical in the neutral compound **1**, one electron oxidation of which results in the oxidation of $L^H{}_{IS}{}^{\bullet-}$ furnishing the coordinated iminobenzoquinone ($L^H{}_{IQ}$) to the VO^{2+} ion. In $\mathbf{1}^+$, the alpha spin density is localized on the oxidovanadium ion, thus omitting the possibility of $VO^{3+}-L^H{}_{IS}{}^{\bullet-}$ coordination (type IV), so far not reported in literature. The quinoidal distortion of the phenyl ring and much shorter C(1)−N(1) (1.312 Å) and O(2)−C(6) (1.248 Å) lengths are consistent with the iminobenzoquinone structure of the coordinated aminophenol in $\mathbf{1}^+$ ion. Expectedly, both calculated V(1)−N(1) and V(1)−O(2) distances are comparatively longer in the cation. It is noted that the bond parameters of the tridentate diimine ligand do not change in the $\mathbf{1}^+$ ion significantly.

*$[(L_1{}^{\bullet2-})(VO^{3+})(L^H{}_{AP}{}^{2-})]^-$ (**1**$^-$) (Type I Coordination).* The spin density distribution in the anion ($\mathbf{1}^-$) is unexpected. The anion $\mathbf{1}^-$ is best described as $[(L_1{}^{\bullet2-})(VO^{3+})(L^H{}_{IS}{}^{2-})]^-$, which incorporates a diimine anion radical and an OV^V ion as shown in Scheme 1. The alpha spin density is localized in the tridentate diimine ligand (Figure 9). The calculation does not show any quinoidal distortion of the phenyl ring of the *o*-aminophenol ligand. Reduction of the iminobenzosemiquinonate anion radical ($L^H{}_{IS}{}^{\bullet-}$) to the dianionic amidophenolato ($L^H{}_{AP}{}^{2-}$) ligand

dx.doi.org/10.1021/ic102296p |*Inorg. Chem.* 2011, 50, 2488–2500

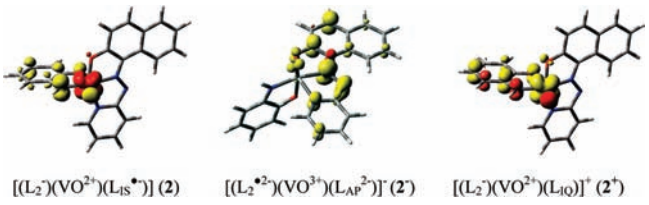

Figure 10. Spin density plot of **2**, $\mathbf{2}^-$, and $\mathbf{2}^+$ (yellow, α spin; red, β spin) and values from Mulliken spin population analyses (spin density, **2**: V, −0.73, N1, 0.26, O2, 0.11, O1, 0.11, C4, 0.10, C6, 0.08. $\mathbf{2}^-$: N2, 0.10, N3, 0.14, N4, 0.31, C20, 0.18, C22, 0.15. $\mathbf{2}^+$:V, 0.87).

results in the transfer of an uncoupled d^1 electron of OV^{IV} to the diimine fragment of the tridentate (L_1^-) ligand furnishing a coordinated diimine anion radical ($L_1^{2-\bullet}$). *This finding shows that the VO^{2+}−amidophenolato ($L^H_{AP}{}^{2-}$) coordinated fragment is strongly reducing and is unstable in solution. So far, a single species of VO^{2+}−amidophenolato ($L^H_{AP}{}^{2-}$) or catecholate (2−) coordination* (type II) *have been reported in the literature.* On the other hand, it augments the experimental findings of formation of only VO^{3+}−amidophenolato ($L^H_{AP}{}^{2-}$) or catecholate (2−) complexes (type I) by reacting VO^{2+} with amidophenolate ($L^H_{AP}{}^{2-}$) or catecholate (2−) ligands. In conjunction with the spin density distribution and bond parameters of both tridentate and bidentate ligands, formulation of $\mathbf{1}^-$ is convincing. The bond distances of the diimine fragment are different from those calculated in **1** and $\mathbf{1}^+$. In $\mathbf{1}^-$, the C═N distance, 1.350 Å, is longer than those in **1** (1.302 Å) and $\mathbf{1}^+$ (1.305 Å). This trend of length of the diimine fragment corroborates well to the formation of the diimine anion radical ($L_1^{\bullet 2-}$), bond parameters of which are well established in many transition metal diimine coordination compounds by experimental and theoretical studies by Wieghardt et al.[29]

*Compounds **2**, $\mathbf{2}^+$, and $\mathbf{2}^-$.* The similar features have been established in the calculations of **2**, $\mathbf{2}^+$ and 2− as shown in Scheme 1. The monoanionic tridentate azo ligand in **2** and **3** is more π-acidic than the tridentate diimine ligand in **1**. Experimentally, it has been observed that the electron transfer events in **2** and **3** are more reversible, and thus, electronic structures of $\mathbf{2}^+$ and 2−, although not isolable, have been elucidated by DFT calculations.

*$(L_2^-)(VO^{2+})(L^H_{IS}{}^{\bullet-})$ (**2**) (Type III Coordination).* The BS (1,1) $M_s = 0$ solution (type III coordination) of **2** is stabilized by 7.14 and 24.42 KJ/mol compared to the closed shell singlet (type I coordination) and the triplet (S = 1, type III coordination) solutions, respectively. The bond parameters of the BS (1,1) $M_s = 0$ state and open shell triplet ($M_S = 1$) solutions are listed in Table 4. The calculated bond parameters of the triplet ($M_S = 1$) state do not correlate with experimental lengths, but the bond parameters of the BS (1,1) $M_s = 0$ state of **2** are consistent with those found in the single-crystal X-ray structure of **3**•1/2 L^{Me}_{AP} and favor the spin-coupled ground state of **2** and **3**•1/2 L^{Me}_{AP}, incorporating one electron paramagnetic VO^{2+} and one electron paramagnetic $L^R_{IS}{}^{\bullet-}$ (type III coordination) as shown in panel (b) of Figure 5. Mulliken spin density distributions are shown in Figure 10, which confirm the localization of spin density only on vanadium (beta) and the aminophenol fragment (alpha spin) only. Experimental bond lengths have been reproduced well by this BS (1,1) $M_s = 0$ state (Table 4). The calculated comparatively shorter C(1)−N(1) (1.365 Å) and O2−C6 (1.299 Å) lengths and a quinoidal distortion of the aromatic phenyl ring with the adjacent long−short−long−short C−C bonds (Table 4, Figure 5) support the presence of $L^H_{IS}{}^{\bullet-}$ in **2** as in **1**.

$[(L_2^-)(VO^{2+})(L^H_{IQ})]^+$ ($\mathbf{2}^+$) (Type V Coordination). The spin density distribution (Figure 10) explains the $[(L_2^-(VO^{2+})(L^H_{IQ})]^+$ description (coordination V) of the $\mathbf{2}^+$ cation as a diamagnetic *o*-iminobenzoquinone (L^H_{IQ}) coordinated to the one electron paramagnetic VO^{2+} core as shown in Scheme 1. Similar to $\mathbf{1}^+$, it also disfavors the hither-to-unknown $VO^{3+}-L_{IS}^{\bullet-}$ (type IV) coordination. The alpha spin density is localized mainly on the oxidovanadium ion. Shorter C(1)−N(1) (1.313 Å) and O(2)−C(6) (1.248 Å) lengths and a quinoidal distortion of the phenyl ring are consistent with the iminobenzoquinone structure of the coordinated *o*-aminophenolate ligand in $\mathbf{2}^+$ ion.

$[(L_2^{\bullet 2-})(VO^{3+})(L^H_{AP}{}^{2-})]^-$ ($\mathbf{2}^-$) (Type I Coordination). Similar to $\mathbf{1}^-$, in $\mathbf{2}^-$, the spin density is distributed on the tridentate NNO-donor ligand (Figure 10). In $\mathbf{2}^-$, it is mainly localized on the azo function making the tridentate ligand a dianionic azo anion radical. The anion $\mathbf{2}^-$ is best described as $[(L_2^{\bullet 2-}(VO^{3+})(L^H_{IS}{}^{2-})]^-$, which incorporates an azo anion radical and *o*-amidophenolato ($L^H_{AP}{}^{2-}$) ligand coordinated to a V^VO ion (type I coordination). The calculation does not show any quinoidal distortion of the phenyl ring of the o-aminophenol ligand. Similar to **1**, $V^{IV}O$−amidophenolato coordination (type II) reduces the azo function of the L_2 ligand furnishing a coordinated azo anion radical ($L_2^{\bullet 2-}$) and type I coordination. The N═N distance in $\mathbf{2}^-$, 1.332 Å, is longer than those in **2** (1.291 Å) and $\mathbf{2}^+$ (1.292 Å) and is consistent with azo anion radical formation.[30] Optimization of the first excited state of $\mathbf{2}^-$ to establish the type II coordination as in $[(L_2^{1-})(VO^{2+})(L^H_{AP}{}^{2-})]^-$ results in type III coordination, incorporating dianionic azo anion radical ($L_2^{\bullet 2-}$) and iminobenzosemiquinonate anion radical as in $[(L_2^{\bullet 2-})(VO^{2+})(L^H_{IS}{}^{\bullet-})]^-$.

The change of electronic states of the oxidovanadium ion (VO^{n+}) and the coordinated ligands in **1**, $\mathbf{1}^+$, $\mathbf{1}^-$ and **2**, $\mathbf{2}^+$, $\mathbf{2}^-$ are unprecedented. The VO^{2+} state is only stable in the presence of the iminobenzosemiquinonate anion radical ($L^R_{IS}{}^{\bullet-}$). Calculations show that in the cations VO^{2+} is present, but the compounds are not isolable. Even after reduction, the VO^{2+} state does not exist in $\mathbf{1}^-$ or $\mathbf{2}^-$, rather it forms diimine or azo anion radicals ($L_1^{\bullet 2-}$ and $L_2^{\bullet 2-}$) itself being oxidized to the VO^{3+}, informing the instability of the OV^{IV} core in absence of $L^R_{IS}{}^{\bullet-}$. In this context, the notably shorter $V-N_{iminosemiquinonate}$ and $V-O_{iminosemiquinonate}$ lengths in **1**•3/2MeOH and **3**•1/2 L^{Me}_{AP} are significant, prompting the higher binding ability of the one electron paramagnetic iminobenzosemiquinonate anion radical ($L^H_{IS}{}^{\bullet-}$) to the one electron paramagnetic VO^{2+} core. Thus, only isolated stable complexes **1**•3/2MeOH, **2**, and **3**•1/2 L^{Me}_{AP} are with type III coordination having a spin-coupled ground state (S = 0).

4. CONCLUSIONS

So far, unexplored coordination chemistry of redox noninnocent *o*-aminophenols (L^R_{AP}, R = H, Me) with a redox non-innocent VO^{n+} (n = 2 or 3) core has been investigated. Deprotonated *o*-aminophenolates can coordinate to VO^{n+} cores having the following electronic structures: (i) dianionic *o*-amidophenolates ($L^R_{AP}{}^{2-}$) coordinated to VO^{3+} core (S = 0) (type I), (ii) dianionic *o*-amidophenolate ($L^R_{AP}{}^{2-}$) coordinated to VO^{2+} core (S = 1/2) (type II), (iii) *o*-iminobenzosemiquinonate anion radicals ($L^R_{IS}{}^{\bullet-}$) coordinated to VO^{2+} core (S = 0 or 1) (type III), (iv) *o*-iminobenzosemiquinonate anion radicals ($L^R_{IS}{}^{\bullet-}$) coordinated to VO^{3+} core (S = 1/2) (type IV), and (v) *o*-iminobenzoquinone (L^R_{IQ}) coordinated to VO^{2+} core (S = 1/2) (type V). But so far, not a single species of oxidovanadium

dx.doi.org/10.1021/ic102296p |*Inorg. Chem.* 2011, 50, 2488–2500

(VO^{n+}) incorporating $L^{R}_{AP}{}^{2-}$, $L^{R}_{IS}{}^{\bullet-}$, or L^{R}_{IQ} has been reported in the literature. In this work, we have disclosed the coordination *o*-aminophenols (L^{R}_{AP}) to VO^{n+} cores by reporting type III coordination as in $(L_1{}^{-})(VO^{2+})(L^{H}_{IS}{}^{\bullet-})\bullet 3/2MeOH$ (**1**•3/2MeOH), $(L_2{}^{-})(VO^{2+})(L^{H}_{IS}{}^{\bullet-})$ (**2**), and $(L_2{}^{-})(VO^{2+})(L^{Me}_{IS}{}^{\bullet-})\bullet 1/2\, L^{Me}_{AP}$ (**3**•1/2 L^{Me}_{AP}) to those incorporate *o*-imino-*p*-*R*-benzosemiquinonate anion radicals ($L^{R}_{IS}{}^{\bullet-}$) and tridentate monoanionic NNO-donor ligands, $L_1{}^{-}$ or $L_2{}^{-}$ {L_1H = (2-[(phenylpyridin-2-yl-methylene)amino]phenol; L_2H = 1-(2-pyridylazo)-2-naphthol; $L^{H}_{IS}{}^{\bullet-}$ = *o*-iminobenzosemiquinonate anion radical; $L^{Me}_{IS}{}^{\bullet-}$ = *o*-imino-*p*-methylbenzosemiquinonate anion radical; L^{Me}_{AP} = *o*-amino-*p*-methylphenol}. Both experimental data and BS-DFT calculations have established that the VO^{2+} state is stable in these complexes in the presence of organic anion radicals. Higher affinity of the one electron paramagnetic VO^{2+} ion toward the iminobenzosemiquinonate anion radical has been reflected in the very short $V^{IV}-N_{iminobenzosemiquinonate}$ bond lengths. The spectroelectrochemical experiments have revealed that the uncoupled VO^{2+} cores are unstable in solutions in one electron reduced $[(L_2{}^{\bullet 2-})(VO^{3+})(L^{R}_{AP}{}^{2-})]^{-}$ and one electron oxidized $[(L_2{}^{-})(VO^{2+})(L^{R}_{IQ})]^{+}$ complexes. DFT calculations show that reduction of the coordinated $L^{R}_{IS}{}^{\bullet-}$ to $L^{R}_{AP}{}^{2-}$ results in the transfer of the uncoupled VO^{2+} electron to a diimine/azo fragment rendering a VO^{3+} core and diimine/azo anion radical. These findings are significant and open up a new area of research to stabilize a paramagnetic VO^{2+} unit with the support of a paramagnetic chelate.

■ ASSOCIATED CONTENT

Supporting Information. X-ray crystallographic CIF files for the complexes **1**•3/2MeOH and **3**•1/2 L^{Me}_{AP}. These materials are available free of charge via the Internet at http://pubs.acs.org.

■ AUTHOR INFORMATION

Corresponding Author

*Email: ghoshp_chem@yahoo.co.in. Phone: +91-33-2428-7017. Fax: +91-33-2477-3597.

■ ACKNOWLEDGMENT

Financial supports received from CSIR, New Delhi, (01(1957)/04/EMR-II) and DST, New Delhi, (SR/S1/IC-10/2008) have been acknowledged. A.S.R. gratefully acknowledges CSIR for SRF(Ex.) (8/531(003)2010-EMR-I) and P.S. acknowledges RKMRC for fellowships.

■ REFERENCES

(1) (a) Rehder, D. *Bioinorganic Vanadium Chemistry*; John Wiley & Sons, Ltd.: New York, 2008. (b) Rehder, D. *Org. Biomol. Chem.* **2008**, *6*, 957–964. (c) Crans, D. C.; Smee, J. J.; Gaidamauskas, E.; Yang, L. *Chem. Rev.* **2004**, *104*, 849–902. (d) Michibata, H.; Yamaguchi, N.; Uyama, T.; Ueki, T. *Coord. Chem. Rev.* **2003**, *237*, 41–51. (e) Smith, T. S., II; LoBrutto, R.; Pecoraro, V. L. *Coord. Chem. Rev.* **2002**, *228*, 1–18. (f) Thompson, K. H.; Orvig, C. *Coord. Chem. Rev.* **2001**, *219*−*221*, 1033–1053. (g) Rehder, D. *Coord. Chem. Rev.* **1999**, *182*, 297–322. (h) Taylor, S. W.; Kammerer, B.; Bayer, E. *Chem. Rev.* **1997**, *97*, 333–346. (i) Rehder, D. *Met. Ions Biol. Syst.* **1995**, *31*, 1–43. (j) Crans, D. C. *Comments Inorg. Chem.* **1994**, *16*, 1–33. (k) Butler, A.; Carrano, C. *J. Coord. Chem. Rev.* **1991**, *109*, 61–105. (l) Rehder, D. *Angew. Chem., Int. Ed. Engl.* **1991**, *30*, 148–167. (m) Nielsen, F. H.; Uthus, E. O. *In Vanadium in Biological Systems*; Chasteen, N. D., Ed.; Kluwer Academic Publishers: Boston, 1990.

(2) (a) Schneider, C. J.; Pecoraro, V. L.*Vanadium: The Versatile Metal*; ACS Syposium Series 974; American Chemical Society: Washington, DC, 2007; pp 148−162. (b) Schneider, C. J.; Zampella, G.; Greco, C.; Pecoraro, V. L.; Gioia, L. D. *Eur. J. Inorg. Chem.* **2007**, *4*, 515–523. (c) Wikete, C.; Wu, P.; Zampella, G.; Gioia, L. D.; Licini, G.; Rehder, D. *Inorg. Chem.* **2007**, *46*, 196–207. (d) Zampella, G.; Fantucci, P.; Pecoraro, V. L.; Gioia, L. D. *Inorg. Chem.* **2006**, *45*, 7133–7143. (e) Raugei, S.; Carloni, P. *J. Phys. Chem. B* **2006**, *110*, 3747–3758. (f) Zampella, G.; Fantucci, P.; Pecoraro, V. L.; Gioia, L. D. *J. Am. Chem. Soc.* **2005**, *127*, 953–960. (g) Kravitz, J. Y.; Pecoraro, V. L. *Pure Appl. Chem.* **2005**, *77*, 1595–1605. (h) Carter-Franklin, J. N.; Butler, A. *J. Am. Chem. Soc.* **2004**, *126*, 15060–15066. (i) Časný, M.; Rehder, D. *Dalton Trans.* **2004**, 839–846. (j) Christmann, U.; Dau, H.; Haumann, M.; Kiss, E.; Liebisch, P.; Rehder, D.; Santoni, G.; Schulzke, C. *Dalton Trans.* **2004**, 2534–2540. (k) Zampella, G; Kravitz, J. Y.; Webster, C. E.; Fantucci, P.; Hall, M. B.; Carlson, H. A.; Pecoraro, V. L.; Gioia, L. D. *Inorg. Chem.* **2004**, *43*, 4127–4136. (l) Smith, T. S., II; Pecoraro, V. L. *Inorg. Chem.* **2002**, *41*, 6754–6760. (m) Isupov, M. N.; Dalby, A. R.; Brindley, A. A.; Izumi, Y.; Tanabe, T.; Murshudov, G. N.; Littlechild, J. A. *J. Mol. Biol.* **2000**, *299*, 1035–1049. (n) Slebodnick, C.; Hamstra, B. J.; Pecoraro, V. L. *Struct. Bonding (Berlin)* **1997**, *89*, 51–108. (o) Butler, A.; Walker, J. V. *Chem. Rev.* **1993**, *93*, 1937–1944.

(3) (a) Rehder, D. *Inorg. Chem. Commun.* **2003**, *6*, 604–617. (b) Eady, R. R. *Coord. Chem. Rev.* **2003**, *237*, 23–30. (c) Rehder, D. *J. Inorg. Biochem.* **2000**, *80*, 133–136. (d) Fay, A. W.; Blank, M. A.; Lee, C. C.; Hu, Y.; Hodgson, K. O.; Hedman, B.; Ribbe, M. W. *J. Am. Chem. Soc.* **2010**, *132*, 12612–12618. (e) Ye, S.; Neese, F.; Ozarowski, A.; Smirnov, D.; Krzystek, J.; Telser, J.; Liao, J. -H.; Hung, C.-H.; Chu, W.-C.; Tsai, Y.-F.; Wang, R. -C.; Chen, K.-Y.; Hsu, H.-F. *Inorg. Chem.* **2010**, *49*, 977–988.

(4) (a) Hamada, T.; Asanuma, M.; Ueki, T.; Hayashi, F.; Kobayashi, N.; Yokoyama, S.; Michibata, H.; Hirota, H. *J. Am. Chem. Soc.* **2005**, *127*, 4216–4222. (b) Kustin, K.; McLeod, G. C.; Gilbert, T. R.; Briggs, L. B. R. T. *Struct. Bonding (Berlin)* **1983**, *53*, 139–160. (c) Smith, M. J.; Ryan, D. E.; Nakanishi, K.; Frank, P.; Hodgson, K. O. *Met. Ions Biol. Syst.* **1995**, *31*, 423–490. (e) Michibata, H.; Uyama, T.; Ueki, T.; Kanamori, K. *Microsc. Res. Tech.* **2002**, *56*, 421–434.

(5) (a) Thompson, K. H.; Lichter, J.; LeBel, C.; Scaife, M. C.; McNeill, J. H.; Orvig, C. *J. Inorg. Biochem.* **2009**, *103*, 554–558. (b) Maurya, M. R.; Agarwal, S.; Abid, M.; Azam, A.; Bader, C.; Ebel, M.; Rehder, D. *Dalton Trans.* **2006**, 937–947. (c) Thompson, K. H.; Liboiron, B. D.; Hanson, G. R.; Orvig, C. *Medicinal Inorganic Chemistry*; ACS Symposium Series 903; American Chemical Society: Washington, DC, 2005; pp 384−399. (d) Thompson, K. H.; McNeill, J. H.; Orvig, C. *Chem. Rev.* **1999**, *99*, 2561–2572. (e) Tracey, A. S.; Crans, D. C. *Vanadium Compounds*; ACS Symposium Series 711; American Chemical Society: Washington, DC, 1998; pp 308−315. (f) Etcheverry, S. B.; Crans, D. C.; Keramidas, A. D.; Cortizo, A. M. *Arch. Biochem. Biophys.* **1997**, *338*, 7–14.

(6) (a) Hamilton, E. E.; Fanwick, P. E.; Wilker, J. J. *J. Am. Chem. Soc.* **2006**, *128*, 3388–3395. (b) Messmore, J. M.; Raines, R. T. *J. Am. Chem. Soc.* **2000**, *122*, 9911–9916. (c) Crans, D. C.; Keramidas, A. D.; Drouza, C. *Phosphorus, Sulfur Silicon Relat. Elem.* **1996**, *109*−*110*, 245–248. (d) Chasteen, N. D. *Struct. Bonding (Berlin)* **1983**, *53*, 105–138.

(7) Representative references are: (a) Chruscinska, E. L.; Micera, G.; Garribba, E. *Inorg. Chem.* **2011**, *50*, 0000. (b) Islam, M. N.; Kumbhar, A. A.; Kumbhar, A. S.; Zeller, M.; Butcher, R. J.; Dusane, M. B.; Joshi, B. N. *Inorg. Chem.* **2010**, *49*, 8237–8246. (c) Nilsson, J.; Degerman, E.; Haukka, M.; Lisensky, G. C.; Garribba, E.; Yoshikawa, Y.; Sakurai, H.; Enyedy, E. A.; Kiss, T.; Hossein, E.; Rehder, D.; Nordlander, E. *Dalton Trans.* **2009**, 7902–7911. (d) Geethalakshmi, K. R.; Waller, M. P.; Thiel, W.; Buhl, M. *J. Phys. Chem. B* **2009**, *113*, 4456–4465. (e) Esbak, H.; Enyedy, E. A.; Kiss, T.; Yoshikawa, Y.; Sakurai, H.; Garribba, E.; Rehder, D. *J. Inorg. Biochem.* **2009**, *103*, 590–600. (f) Mba, M.; Pontini, M.; Lovat, S.; Zonta, C.; Bernardinelli, G.; Kundig, P. E.; Licini, G. *Inorg. Chem.* **2008**, *47*, 8616–8618. (g) Wu, P.; Çelik, C.; Santoni, G.; Dallery, J.; Rehder, D. *Eur. J. Inorg. Chem.* **2008**, 5203–5213. (h) Maurya, M. R.; Kumar, A.; Ebel, M.; Rehder, D. *Inorg. Chem.* **2006**, *45*, 5924–5937. (i) Less, G. B.; Ockwig, N. W.; Rasmussen, P. G. *Inorg. Chem.* **2006**, *45*, 7105–7110. (j) Feiters,

M. C.; Leblanc, C.; Küpper, F. C.; Meyer-Klaucke, W.; Michel, G.; Potin, P. *J. Am. Chem. Soc.* **2005**, *127*, 15340–15341. (k) Wong, S. Y.; Sun, R. W. -Y.; Chung, N. P.-Y.; Lin, C. L.; Che, C. M. *Chem. Commun.* **2005**, 3544–3546. (l) Hinnemann, B.; Nørskov, J. K. *J. Am. Chem. Soc.* **2003**, *125*, 1466–1467. (m) Gätjens, J.; Meier, B.; Kiss, T.; Nagy, E. M.; Buglyó, P.; Sakurai, H.; Kawabe, K.; Rehder, D. *Chem.—Eur. J.* **2003**, *9*, 2924–2935. (n) Santoni, G.; Licini, G. M.; Rehder, D. *Chem.—Eur. J.* **2003**, *9*, 4700–4708. (o) Rehder, D.; Pessoa, J. C.; Geraldes, C. F. G. C.; Kabanos, T.; Kiss, T.; Meier, B.; Micera, G.; Pettersson, L.; Rangel, M.; Salifoglou, A.; Turel, I.; Wang, D. *J. Biol. Inorg. Chem.* **2002**, *7*, 384–396. (p) Slebodnick, C.; Hamstra, B. J.; Pecoraro, V. L. *Modelling the Biological Chemistry of Vanadium: Structural and Reactivity Studies Elucidating Biological Function: Structure and Bonding*; Sadler, P., Ed.; Springer: Berlin, 1997, 89, 57.

(8) (a) Baruah, B.; Das, S.; Chakravorty, A. *Inorg. Chem.* **2002**, *41*, 4502–4508. (b) Cornman, C. R.; Kampf, J.; Pecoraro, V. L. *Inorg. Chem.* **1992**, *31*, 1981–1983. (c) Cornman, C. R.; Colpas, G. J.; Hoeschele, J. D.; Kampf, J.; Pecoraro, V. L. *J. Am. Chem. Soc.* **1992**, *114*, 9925–9933. (d) Cooper, S. R.; Koh, Y. B.; Raymond, K. N. *J. Am. Chem. Soc.* **1982**, *104*, 5092–5102.

(9) (a) Drouza, C.; Keramidas, A. D. *Inorg. Chem.* **2008**, *47*, 7211–7224. (b) Drouza, C.; Tolis, V.; Gramlich, V.; Raptopoulou, C.; Terzis, A.; Sigalas, M. P.; Kabanos, T. A.; Keramidas, A. D. *Chem. Commun.* **2002**, 2786–2787.

(10) (a) Chun, H.; Verani, C. N.; Chaudhuri, P.; Bothe, E.; Bill, E.; Weyhermüller, T.; Wieghardt, K. *Inorg. Chem.* **2001**, *40*, 4157–5166. (b) Mukherjee, C.; Weyhermüller, T.; Bothe, E.; Chaudhuri, P. *Inorg. Chem.* **2008**, *47*, 11620–11632.

(11) Rowe, R. A.; Jones, M. M. *Inorg. Synth.* **1957**, *5*, 113–115.

(12) (a) Sheldrick, G. M. *ShelXS97*; Universität Göttingen: Göttingen, Germany, 1997. (b) Sheldrick, G. M. *ShelXL97*; Universität Göttingen: Göttingen, Germany, 1997.

(13) Frisch, M. J.; Trucks, G. W.; Schlegel, H. B.; Scuseria, G. E.; Robb, M. A.; Cheeseman, J. R.; Montgomery, Jr., J. A.; Vreven, T.; Kudin, K. N.; Burant, J. C.; Millam, J. M.; Iyengar, S. S.; Tomasi, J.; Barone, V.; Mennucci, B.; Cossi, M.; Scalmani, G.; Rega, N.; Petersson, G. A.; Nakatsuji, H.; Hada, M.; Ehara, M.; Toyota, K.; Fukuda, R.; Hasegawa, J.; Ishida, M.; Nakajima, T.; Honda, Y.; Kitao, O.; Nakai, H.; Klene, M.; Li, X.; Knox, J. E.; Hratchian, H. P.; Cross, J. B.; Bakken, V.; Adamo, C.; Jaramillo, J.; Gomperts, R.; Stratmann, R. E.; Yazyev, O.; Austin, A. J.; Cammi, R.; Pomelli, C.; Ochterski, J. W.; Ayala, P. Y.; Morokuma, K.; Voth, G. A.; Salvador, P.; Dannenberg, J. J.; Zakrzewski, V. G.; Dapprich, S.; Daniels, A. D.; Strain, M. C.; Farkas, O.; Malick, D. K.; Rabuck, A. D.; Raghavachari, K.; Foresman, J. B.; Ortiz, J. V.; Cui, Q.; Baboul, A. G.; Clifford, S.; Cioslowski, J.; Stefanov, B. B.; Liu, G.; Liashenko, A.; Piskorz, P.; Komaromi, I.; Martin, R. L.; Fox, D. J.; Keith, T.; Al-Laham, M. A.; Peng, C. Y.; Nanayakkara, A.; Challacombe, M.; Gill, P. M. W.; Johnson, B.; Chen, W.; Wong, M. W.; Gonzalez, C.; Pople, J. A. *Gaussian 03*, revision E.01; Gaussian, Inc.: Wallingford, CT, 2004.

(14) (a) Hohenberg, P.; Kohn, W. *Phys. Rev.* **1964**, *136*, B864–B871. (b) Kohn, W.; Sham, L. *J. Phys. Rev.* **1965**, *140*, A1133–A1138. (c) Parr, R. G.; Yang, W. *Density Functional Theory of atoms and molecules*; Oxford University Press: Oxford, U.K., 1989. (d) Salahub, D. R.; Zerner, M. C. *The Challenge of d and f Electrons*; ACS Symposium Series 394; American Chemical Society: Washington, DC, 1989.

(15) (a) Becke, A. D. *J. Chem. Phys.* **1993**, *98*, 5648–5652. (b) Lee, C.; Yang, W.; Parr, R. G. *Phys. Rev. B* **1988**, *37*, 785–789. (c) Miehlich, B.; Savin, A.; Stoll, H.; Preuss, H. *Chem. Phys. Lett.* **1989**, *157*, 200–205. (d) Bruke, K.; Perdew, J. P.; Wang, Y. *Electronic Density Functional Theory: Recent Progress and New Direction*; Dobson, J. F., Vignale, G., Das, M. P., Eds.; Plenum: New York, 1998. (e) Perdew, J. P. *Electronic Structure of Solids, '91*; Ziesche, P, Eschrig, H., Eds.; Akademie Verlag: Berlin, 1991. (f) Perdew, J. P.; Chevary, J. A.; Vosko, S. H.; Jackson, K. A.; Pederson, M. R.; Sing, D. J.; Fiolhais, C. *Phys. Rev.* **1992**, *B 46*, 6671–6687. (g) Perdew, J. P.; Chevary, J. A.; Vosko, S. H.; Jackson, K. A.; Pederson, M. R.; Sing, D. J.; Fiolhais, C. *Phys. Rev.* **1993**, *B 48*, 4978–4978. (h) Perdew, J. P.; Bruke, K.; Wang, Y. *Phys. Rev.* **1996**, *B 54*, 16533–16539. (i) Perdrew, J. P.; Burke, K.; Ernzerhof, M. *Phys. Rev. Lett.* **1996**, *77*, 3865–3868. (j) Perdew, J. P.; Burke, K.; Ernzerhof, M. *Phys. Rev. Lett.* **1997**, *78*, 1396–1396. (k) Perdew, J. P.; Ernzerhof, M.; Burke, K. *J. Chem. Phys.* **1996**, *105*, 9982–9985. (l) Ernzerhof, M.; Scuseria, G. E. *J. Chem. Phys.* **1999**, *110*, 5029–5036.

(16) Pulay, P. *J. Comput. Chem.* **1982**, *3*, 556–560.

(17) Schlegel, H. B.; McDouall, J. J. In *Computational Advances in Organic Chemistry*; Ogretir, C., Csizmadia, I. G., Eds.; Kluwer Academic: The Netherlands, 1991; pp 167−185.

(18) (a) Hay, P. J.; Wadt, W. R. *J. Chem. Phys.* **1985**, *82*, 270–283. (b) Wadt, W. R.; Hay, P. J. *J. Chem. Phys.* **1985**, *82*, 284–298. (c) Hay, P. J.; Wadt, W. R. *J. Chem. Phys.* **1985**, *82*, 299–310.

(19) (a) Petersson, G. A.; Bennett, A.; Tensfeldt, T. G; Al-Laham, M. A.; Shirley, W. A.; Mantzaris, J. *J. Chem. Phys.* **1988**, *89*, 2193–2218. (b) Petersson, G. A.; Al-Laham, M. A. *J. Chem. Phys.* **1991**, *94*, 6081–6090.

(20) (a) Hehre, W. J.; Ditchfield, R.; Pople, J. A. *J. Chem. Phy.* **1972**, *56*, 2257–2261. (b) Hariharan, P. C.; Pople, J. A. *Theo. Chim. Acta.* **1973**, *28*, 213–222. (c) Hariharan, P. C.; Pople, J. A. *Mol. Phys.* **1974**, *27*, 209–214. (d) Rassolov, V. A.; Ratner, M. A.; Pople, J. A.; Redfern, P. C.; Curtiss, L. A. *J. Comput. Chem.* **2001**, *22*, 976–984. (e) Francl, M. M.; Pietro, W. J.; Hehre, W. J.; Binkley, J. S.; DeFrees, D. J.; Pople, J. A.; Gordon, M. S. *J. Chem. Phys.* **1982**, *77*, 3654–3665.

(21) (a) Bauernschmitt, R.; Ahlrichs, R. *Chem. Phys. Lett.* **1996**, *256*, 454–464. (b) Stratmann, R. E.; Scuseria, G. E.; Frisch, M. *J. Chem. Phys.* **1998**, *109*, 8218–8224. (c) Casida, M. E.; Jamorski, C.; Casida, K. C.; Salahub, D. R. *J. Chem. Phys.* **1998**, *108*, 4439–4449.

(22) The results will be published elsewhere.

(23) (a) Mondal, S.; Ghosh, P.; Chakravorty, A. *Inorg. Chem.* **1997**, *36*, 59–63. (b) Mondal, S.; Ghosh, P.; Chakravorty, A. *Indian J. Chem.* **1996**, *35A*, 171–174. (c) Dutta, S.; Mondal, S.; Chakravorty, A. *Polyhedron* **1995**, *14*, 1163–1168. (d) Mondal, S.; Rath, S. P.; Dutta, S.; Chakravorty., A. *Dalton Trans.* **1996**, 99–103. (e) Mondal, S.; Dutta, S.; Chakravorty, A. *Dalton Trans.* **1995**, 1115–1120. (f) Chakravarty, J.; Dutta, S.; Chandra, S. K.; Basu, P.; Chakravorty, A. *Inorg. Chem.* **1993**, *32*, 4249–4249.

(24) (a) Chatterjee, P. B.; Bhattacharya, S.; Audhya, A.; Choi, K.-Y.; Endo, A.; Chaudhury, M. *Inorg. Chem.* **2008**, *47*, 4891–4902. (b) Chatterjee, P. B.; Mandal, D.; Audhya, A.; Choi, K.-Y.; Endo, A.; Chaudhury, M. *Inorg. Chem.* **2008**, *47*, 3709–3718. (c) Dutta, S. K.; Samanta, S.; Ghosh, D.; Butcher, R. J.; Chaudhury, M. *Inorg. Chem.* **2002**, *41*, 5555–5560. (d) Chatterjee, P. B.; Kundu, N.; Bhattacharya, S.; Choi, K.-Y.; Endo, A.; Chaudhury, M. *Inorg. Chem.* **2007**, *46*, 5483–5485. (e) Maurya, M. R.; Agarwal, S.; Bader, C.; Ebel, M.; Rehder, D. *Dalton Trans.* **2005**, 537–544. (f) Farahbakhsh, M.; Schmidt, H.; Rehder, D. *Chem. Commun.* **1998**, 2009–2010. (g) Biswas, B.; Weyhermüller, T.; Bill, E.; Chaudhuri, P. *Inorg. Chem.* **2009**, *48*, 1524–1532.

(25) Allen, F. H.; Kennard, O. *Chem. Des. Autom. News* **1993**, *8*, 31–37.

(26) (a) Barroso, S.; Adao, P.; Madeira, F.; Duarte, M. T.; Pessoa, J. C.; Martins, A. M. *Inorg. Chem.* **2010**, *49*, 7452–7463. (b) Ebel, M.; Rehder, D. *Inorg. Chem.* **2006**, *45*, 7083–7090. (c) Groysman, S.; Goldberg, I.; Goldschmidt, Z.; Kol, M. *Inorg. Chem.* **2005**, *44*, 5073–5080. (d) Keramidas, A. D.; Papaioannou, A. B.; Vlahos, A.; Kabanos, T. A.; Bonas, G.; Makriyannis, A.; Rapropoulou, C. P.; Terzis, A. *Inorg. Chem.* **1996**, *35*, 357–367. (e) Bonadies, J. A.; Butler, W. M.; Pecoraro, V. L.; Carrano, C. J. *Inorg. Chem.* **1987**, *26*, 1218–1222. (f) Riley, P. E.; Pecoraro, V. L.; Carrano, C. J.; Bonadies, J. A. *Inorg. Chem.* **1987**, *25*, 154–160.

(27) (a) Verani, C. N.; Gallert, S.; Bill, E.; Weyhermüller, T.; Wieghardt, K.; Chaudhuri, P. *Chem. Commun.* **1999**, 1747–1748. (b) Chaudhuri, P.; Verani, C. N.; Bill, E.; Bothe, E.; Weyhermüller, T.; Wieghardt, K. *J. Am. Chem. Soc.* **2001**, *123*, 2213–2223. (c) Chun, H.; Weyhermüller, T.; Bill, E.; Wieghardt, K. *Angew. Chem., Int. Ed.* **2001**, *40*, 2489–2492. (d) Chun, H.; Chaudhuri, P.; Weyhermüller, P.; Wieghardt, K. *Inorg. Chem.* **2002**, *41*, 790–795. (e) Sun, X.; Chun, H.; Hildenbrand, K.; Bothe, E.; Weyhermüller, T.; Neese, F.; Wieghardt, K. *Inorg. Chem.* **2002**, *41*, 4295–4303. (f) Chun, H.; Bill, E.; Bothe, E.; Weyhermüller, T.; Wieghardt, K. *Inorg. Chem.* **2002**, *41*, 5091–5099.

(g) Min, K. S.; Weyhermüller, T.; Bothe, E.; Wieghardt, K. *Inorg. Chem.* **2004**, *43*, 2922–2931. (h) Min, K. S.; Weyhermüller, T.; Wieghardt, K. *Dalton Trans.* **2004**, 178–186. (i) Kokatam, S. L.; Chaudhuri, P.; Weyhermüller, T.; Wieghardt, K. *Dalton Trans.* **2007**, 373–378.

(28) (a) Das, D.; Mondal, T. K.; Mobin, S. M.; Lahiri, G. K. *Inorg. Chem.* **2009**, *48*, 9800–9810. (b) Das, D.; Das, A. K.; Sarkar, B.; Mondal, T. K.; Mobin, S. M.; Fiedler, J.; Zalis, S.; Urbanos, F. A.; Jimenez-Aparicio, R.; Kaim, W.; Lahiri, G. K. *Inorg. Chem.* **2009**, *48*, 11853–11864. (c) Bhattacharya, S.; Gupta, P.; Basuli, F.; Pierpont, C. G. *Inorg. Chem.* **2002**, *41*, 5810–5816.

(29) (a) Muresan, N.; Chlopek, K.; Weyhermüller, T.; Neese, F.; Wieghardt, K. *Inorg. Chem.* **2007**, *46*, 5327–5337. (b) Muresan, N.; Weyhermüller, T.; Wieghardt, K. *Dalton Trans.* **2007**, 4390–4398. (c) Lu, C. C.; Weyhermüller, T.; Bill, E.; Bothe, E.; Wieghardt, K. *J. Am. Chem. Soc.* **2008**, *130*, 3181–3197. (d) Muresan, N.; Lu, C. C.; Ghosh, M.; Peters, J. C.; Abe, M.; Henling, L. M.; Weyhermüller, T.; Bill, E.; Wieghardt, K. *Inorg. Chem.* **2008**, *47*, 4579–4590. (e) Ghosh, M.; Sproules, S.; Weyhermueller, T.; Wieghardt, K. *Inorg. Chem.* **2008**, *47*, 5963–5970. (f) Ghosh, M.; Weyhermüller, T.; Wieghardt, K. *Dalton Trans.* **2008**, 5149–5151. (g) Khusniyarov, M. M.; Weyhermüller, T.; Bill, E.; Wieghardt, K. *J. Am. Chem. Soc.* **2009**, *131*, 1208–1221. (h) Ghosh, P.; Bill, E.; Weyhermüller, T.; Neese, F.; Wieghardt, K. *J. Am. Chem. Soc.* **2003**, *125*, 1293–1308.

(30) (a) Shivakumar, M.; Pramanik, K.; Ghosh, P.; Chakravorty, A. *Inorg. Chem.* **1998**, *37*, 5968–5969. (b) Shivakumar, M.; Pramanik, K.; Ghosh, P.; Chakravorty, A. *Chem. Commun.* **1998**, 2103–2104. (c) Pramanik, K.; Shivakumar, M.; Ghosh, P.; Chakravorty, A. *Inorg. Chem.* **2000**, *39*, 195–199. (d) Schwach, M.; Hausen, H. D.; Kaim, W. *Inorg. Chem.* **1999**, *38*, 2242–2243. (e) Doslik, N.; Sixt, T.; Kaim, W. *Angew. Chem., Int. Ed. Engl.* **1998**, *37*, 2403–2404. (f) Sanyal, A.; Chatterjee, S.; Castineiras, A.; Sarkar, B.; Singh, P.; Fiedler, J.; Zalis, S.; Kaim, W.; Goswami, S. *Inorg. Chem.* **2007**, *46*, 8584–8593. (g) Samanta, S.; Singh, P.; Fiedler, J.; Záliš, S.; Kaim, W.; Goswami, S. *Inorg. Chem.* **2008**, *47*, 1625–1633. (h) Paul, N.; Samanta, S.; Goswami, S. *Inorg. Chem.* **2010**, *49*, 2649–2655.